Journal of Organometallic Chemistry 888 (2019) 54–64

Contents lists available at ScienceDirect

Journal of Organometallic Chemistry

journal homepage: www.elsevier.com/locate/jorganchem

Synthesis and characterization of iridium hydride complexes with *meso*-$Ph_2PCH_2P(Ph)CH_2P(Ph)CH_2PPh_2$ (*meso*-dpmppm) as an unsymmetric pincer ligand

Tomoaki Tanase*, Natsumi Mori, Kanako Nakamae, Takayuki Nakajima

Department of Chemistry, Faculty of Science, Nara Women's University, Kitauoya-nishi-machi, Nara, 630-8506, Japan

ARTICLE INFO

Article history:
Received 4 February 2019
Received in revised form
4 March 2019
Accepted 13 March 2019
Available online 18 March 2019

Keywords:
Iridium
Hydride
PPP pincer
Tetraphosphine /oxidative addition

ABSTRACT

Reaction of $[IrCl(CO)(PPh_3)_2]$ with *meso*-bis[(diphenylphosphinomethyl)phenylphosphino]methane (*meso*-dpmppm) afforded a mononuclear Ir^I complex, $[Ir(meso\text{-dpmppm}-\kappa^3)(CO)_2]Cl$ (**1**), which showed excellent reactivity towards HX, H_2, HCOOH, and R_3SiH to yield a series of Ir^{III} hydride complexes, $[IrH(meso\text{-dpmppm}-\kappa^3)(CO)_2]X_2$ (X = Cl (**2**), PF_6 (**2***)), $[Ir(H)_2(meso\text{-dpmppm}-\kappa^3)(CO)]Cl$ (**4**), and $[IrH(SiR_3)(meso\text{-dpmppm}-\kappa^3)(CO)]Cl$ ($R_3 = Me_2Ph$ (**5a**), Ph_2H (**5b**)). The hydride Ir^{III} complexes with isocyanides, $[IrH(meso\text{-dpmppm}-\kappa^3)(RNC)_2](PF_6)_2$ (R = Xyl (2,6-xylyl) (**3a**), Mes (2,4,6-mesityl) (**3b**), Cy (cyclohexyl) (**3c**), ^{t}Bu (*tert*-butyl) (**3d**)), were also prepared by reacting $[IrCl(cod)]_2$ with *meso*-dpmppm and RNC in the presence of NH_4PF_6. Complexes **2**–**5** were characterized by ^1H and ^{31}P NMR and ESI–MS spectroscopies and X-ray diffraction analyses (**3a**, **4**, **5a**,**b**) to have distorted octahedral Ir^{III} structures supported by a *meso*-dpmppm in meridional mode as an unsymmetrical *PPP*–κ^3 pincer ligand, coordinating with two outer and one inner phosphorus atoms to form fused six- and four-membered chelate rings and bearing an uncoordinate inner phosphine unit. The terminal hydride occupied the axial open site surrounded by the equatorially oriented phenyl groups of *meso*-dpmppm and is *trans* to the carbonyl (**2**, **4**) and isocyanide ligands (**3**) nested in the closed site with respect to the {Ir(*meso*-dpmppm–κ^3)} pincer plane. The remaining equatorial site is coordinated by CO (**2**), RNC (**3**), hydride (**4**), and silyl (**5**) ligand. These structural features demonstrated that oxidative additions of H^+, H_2, and R_3SiH occurred at the axial open site of **1**. The uncoordinate inner phosphine of **1** is readily reacted with $[Cp^*IrCl_2]_2$ to give $[Ir(\mu\text{–}meso\text{-dpmppm}-\kappa^3)(\eta^5\text{–}Cp^*IrCl_2)(CO)_2]Cl$ (**1**·Cp^*IrCl_2, Cp^* = 1,2,3,4,5-pentamethylcyclopentadienyl), which further transformed by oxidative addition of H_2 and HCl to $[Ir(H)_2(\mu\text{–}meso\text{-dpmppm}-\kappa^3)(\eta^5\text{–}Cp^*IrCl_2)(CO)]Cl$ (**4**·Cp^*IrCl_2) and $[IrH(\mu\text{–}meso\text{-dpmppm}-\kappa^3)(\eta^5\text{–}Cp^*IrCl_2)(CO)_2]Cl_2$ (**2**·Cp^*IrCl_2), respectively, and however addition of bulky Me_2PhSiH resulted in a disproportionation mixture of $[IrH(Me_2PhSi)(\mu\text{–}meso\text{-dpmppm}-\kappa^3)(\eta^5\text{-}Cp^*IrCl_2)(CO)]Cl$ (**5a**·Cp^*IrCl_2) as well as **4**·Cp^*IrCl_2, indicating an allosteric influence by attaching Cp^*IrCl_2 unit on the uncoordinate phosphine of the {Ir(*meso*-dpmppm–κ^3)} unsymmetric pincer unit in **1**.

1. Introduction

A number of pincer ligands, which support a metal center in tridentate meridional mode, have been extensively developed by varying central and lateral donor atoms and their linker units, and have applied to versatile catalytic reactions as late transition-metal complexes [1–3]. While symmetric pincer ligands having two same lateral donor arms on the central donor unit have predominantly been synthesized in the early stage, unsymmetrical pincers with two different terminal donors and/or arms have also been developed to utilize their intelligent multifunctions in many catalytic reactions [4–7]. Among them, number of *PPP* pincer ligands is relatively small owing to soft donating property of the central P atom. As representative examples, $R_2P(CH_2)_2P(R')(CH_2)_2PR_2$ (R = Ph, Ar, ^{t}Bu, Et, Cy; R' = Ph, Et) [8–19], $R_2P(CH_2)_3P(R')(CH_2)_3PR_2$ (R = Ph, ^{i}Pr, Cy; R' = Ph, ^{t}Bu) [20–26], $(R_2P(o\text{-}C_6H_4))_2PX$ (R = ^{i}Pr, Ph; X = O, O^{i}Pr, OMe, Me, H) and $\{(^iPr_2P(o\text{-}C_6H_4))_2P\}^-$ [27–32], Pigiphos [33–35], and so on [36–40] have been reported to act as *PPP* pincer ligands. It should be noted that outstanding studies have recently

* Corresponding author
E-mail address: tanase@cc.nara-wu.ac.jp (T. Tanase).

https://doi.org/10.1016/j.jorganchem.2019.03.010
0022-328X/

been carried out for activation of dinitrogen by using *PPP* pincer complexes with {Mo((^{t}Bu$_2$PCH$_2$CH$_2$)$_2$PPh)} [8] and {Fe((^{i}Pr$_2$P(*o*-C$_6$H$_4$))$_2$PPh)} units [26]. In contrast to the symmetric ones, unsymmetrical *PPP* pincers are extremely limited to only few examples including R$_2$P(CH$_2$)$_2$P(Ph)(CH$_2$)$_3$PR$_2$ (R = Et [18], Ph [41]), Ph$_2$P(CH$_2$)$_2$P(Ph)R (R = 5,6-dimethyl-7-phenyl-7-phosphabicyclo [2.2.1]hept5-ene) [42], and {Ph$_2$P(CH$_2$)$_2$P(Ph)(*o*-C$_6$H$_4$)PPh}$^-$ [43], due to synthetic difficulty.

We have synthesized a series of methylene-bridged linear tetraphosphine ligands, *meso* and *rac*-Ph$_2$PCH$_2$P(Ph)(CH$_2$)$_n$P(Ph)CH$_2$PPh$_2$ (n = 1 (dpmppm) [44–55], 2 (dpmppe) [56], 3 (dpmppp) [56–59]), to organize structurally constrained multinuclear metal centers. Especially, *meso*-dpmppm has been revealed to stabilize versatile molecular metal chains of Pd$_8$ [53–55], Au$_4$ [44,51], Ag$_4$ [45], Cu$_4$ and Cu$_8$ [46], as well as AuAgCu octanuclear rings, [47]. It also supports di- and tetranuclear copper hydride complexes, [Cu$_2$(μ–H)(μ–*meso*-dpmppm)$_2$]$^+$ and [Cu$_4$(μ$_4$–H)(μ–H)$_2$(μ–*meso*-dpmppm)$_2$]$^+$ [51] and nona- and hexadecanuclear CuH clusters, [Cu$_9$(μ–H)$_7$(μ–*meso*-dpmppm)$_3$]$^{2+}$ and [Cu$_{16}$(μ–H)$_{14}$(μ–*meso*-dpmppm)$_4$]$^{2+}$ [60], in various coordination modes. Furthermore, we have recently found that *meso*-dpmppm hold a mononuclear center of Pd^{II} or Pt^{II} in a pincer-type fashion to form a {M(*meso*-dpmppm–κ^3)}$^{2+}$ motif, in which six- and four-membered chelate rings are fused with an uncoordinated phosphine unit involved in the six-membered ring (Scheme 1) [48,61]. The Pd^{II} pincer unit of [PdCl(*meso*-dpmppm–κ^3)]$^+$ is so labile to be easily converted into di- and trinuclear species of [PdCl$_2$(η^5–Cp*MCl$_2$)(μ–*meso*-dpmppm–κ^3,κ^1)], [PdCl$_2$(η^5–Cp*M'Cl$_2$)(η^5–Cp*MCl$_2$)(μ–*meso*-dpmppm–κ^2,κ^1,κ^1)], and [PdCl(μ–Cl)(η^5–Cp*M'Cl)(η^5–Cp*MCl$_2$)(μ–*meso*-dpmppm–κ^2,κ^1,κ^1)]PF$_6$ (M, M' = Ir, Rh), through an addition of {Cp*MCl$_2$} fragment (M = Rh, Ir, Cp* = pentamethylcyclopentadienyl) to the uncoordinated phosphine, which brought about conformational change of the six-membered ring from a stable chair (C) to a twist-boat (T) structure, and further destabilized the strained four-membered chelate ring to open for the third metal ion (Scheme 1) [48]. In contrast, the Pt^{II} analogue, [PtCl(*meso*-dpmppm–κ^3)]$^+$, is very stable and was converted by treating with isocyanides to [Pt(*meso*-dpmppm–κ^3)(RNC)]$^{2+}$ (R = 2,6-xylyl (Xyl), cyclohexyl (Cy)) and then reacted with R'NH$_2$ (R = benzyl (Bn), *n*-octyl (Oct)) to afford *N*-acyclic diamino carbene complexes, [Pt(*meso*-dpmppm–κ^3){C(NHR)(NHR')}]$^{2+}$ (R = Xyl, Cy; R' = Bn, Oct) (Scheme 1) [61]. An attachment of {Cp*IrCl$_2$} unit onto the uncoordinate P atom of [Pt(*meso*-dpmppm–κ^3)(RNC)]$^{2+}$ interestingly prohibited formation

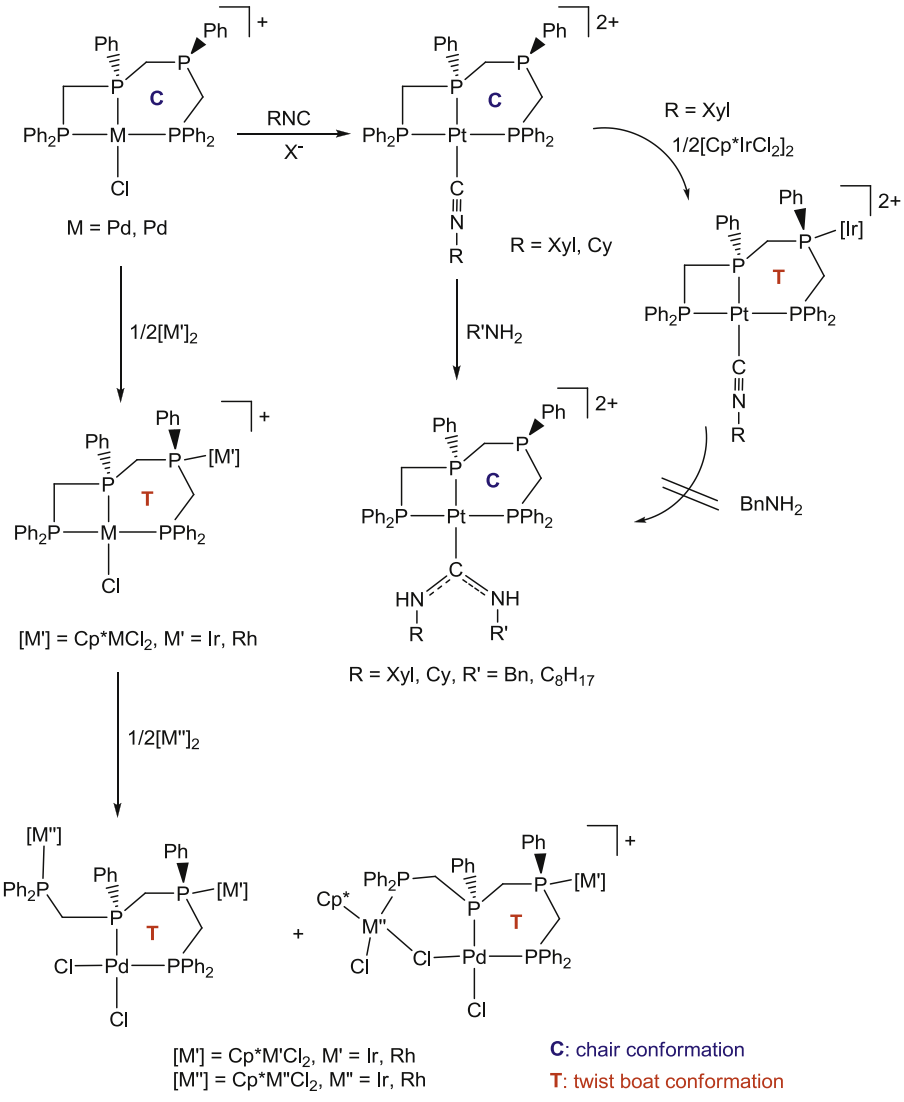

Scheme 1. Reactions of [MCl(*meso*-dpmppm–κ^3)]$^+$ (M = Pd [48], Pt [61]).

of the NAC complex, probably due to conformational change of the six-membered chelate ring from a stable chair to a sterically demanded twist-boat structure.

In the present study, we have tried to synthesize Ir^{I} pincer complexes by utilizing *meso*-dpmppm as an unsymmetrical *PPP* pincer ligand since Ir^{I} pincer complexes generally possess high reducing ability, and wish to report herein synthesis and characterization of an Ir^{I} pincer complex, [Ir(*meso*-dpmppm−κ^3)(CO)$_2$]Cl (**1**) and its reactions with H^+, HCOOH, H_2, and hydrosilanes to afford a series of Ir^{III} hydride complexes supported by *meso*-dpmppm, [IrH(*meso*-dpmppm−κ^3)(CO)$_2$]$^{2+}$ (**2**), [IrH(*meso*-dpmppm−κ^3)(RNC)$_2$]$^{2+}$ (**3**; R = Xyl, Mes (2,4,6-mesityl), Cy, ^{t}Bu (*tert*-butyl)), [Ir(H)$_2$(*meso*-dpmppm−κ^3)(CO)]$^+$ (**4**), and [IrH(SiR$_3$)(*meso*-dpmppm−κ^3)(CO)]$^+$ (**5**; R = Me$_2$Ph, HPh$_2$). Allosteric effect of conformational switch via attaching a {Cp*IrCl$_2$} fragment on the uncoordinate P atom of **1** was also examined based on formation of the Ir^{III} hydride complexes.

2. Results and discussion

2.1. Mononuclear Ir^{I} complex with meso-dpmppm, [Ir(meso-dpmppm−κ^3)(CO)$_2$]Cl (**1**)

When [IrCl(CO)(PPh$_3$)$_2$] was reacted with 1 equiv. of *meso*-dpmppm under CO (1 atm) atmosphere in THF, colorless microcrystals of [Ir(*meso*-dpmppm−κ^3)(CO)$_2$]Cl (**1**) were precipitated quantitatively (Scheme 2), and were characterized by elemental analysis, ^{1}H and ^{31}P{^{1}H} NMR and ESI−MS spectra. Complex **1** could also be obtained by treating [IrCl(coe)]$_2$ with *meso*-dpmppm under CO (1 atm) in THF in 75% yield. The ^{31}P{^{1}H} NMR spectrum of **1** in CD$_2$Cl$_2$ showed four resonances at δ_{PA} −62.2 (dd, $J_{PP'}$ = 174, 80 Hz), δ_{PB} −78.4 (ddd, $J_{PP'}$ = 87, 80, 29 Hz), δ_{PC} −33.6 (dd, $J_{PP'}$ = 87, 73 Hz), and δ_{PD} −17.3 (ddd, $J_{PP'}$ = 174, 73, 29 Hz) (Fig. S5a), which are assignable to P_A, P_B, P_C, and P_D atoms in the light of PP′ coupling constants ($J_{PP'}$) and 2D NMR (^{1}H−^{1}H and ^{31}P−^{31}P COSY and ^{1}H−^{31}P HMBC) techniques (the labels of phosphorus atoms are indicated in Fig. S5). The spectral patterns are reminiscent of those for [PtCl(*meso*-dpmppm−κ^3)]Cl [61], which suggest the asymmetric κ^3*PPP* pincer structure, although the characteristic *trans*-P_AP_D coupling constant of 174 Hz is considerably smaller than is observed in the Pt^{II} complex (419 Hz). Variable temperature ^{31}P{^{1}H} NMR spectra of **1** did not indicate any fluxional behaviors of *meso*-dpmppm-κ^3*PPP* ligand. While the ESI−MS spectrum of **1** in CH$_2$Cl$_2$ (Fig. S9) showed a mono cation peak of [Ir(dpmppm)(CO)]$^+$ at *m*/*z* = 849.226 (*z* = 1), the IR spectrum of **1** as KBr disk give rise to two ν_{CO} peaks at 2004 and 1973 cm^{-1}, which indicate a *cis* geometry of the carbonyl groups and are comparable to those of [Ir(PCP)(CO)$_2$]$^+$ complexes (1971−2068 cm^{-1}, PCP = [C(2-PR$_2$-4-R′-C$_6$H$_3$)$_2$] (R = ^{i}Pr, ^{t}Bu; R' = H, NMe$_2$), 2,6-[(OP^{t}Bu$_2$)$_2$C$_6$H$_3$]$^-$ (= POCOP^{t}Bu), 2,6-[(CH$_2$P(CF$_3$)$_2$)$_2$C$_6$H$_3$]$^-$) [62,63,70], and higher in energy than those of [Ir(PBP)(CO)$_2$]$^+$ (1960, 1913 cm^{-1}, PBP = [B(2-P^{i}Pr$_2$-C$_6$H$_4$)$_2$]$^-$) [64]. By analogy with the Ir^{I} dicarbonyl complexes with the PCP and PBP pincer ligands, complex **1** is estimated to possess a distorted structure in between square pyramidal and trigonal bipyramidal geometry with a meridional *PPP* pincer scaffold of *meso*-dpmppm, which may be consistent with the reduced *trans*-P_AP_D coupling constant.

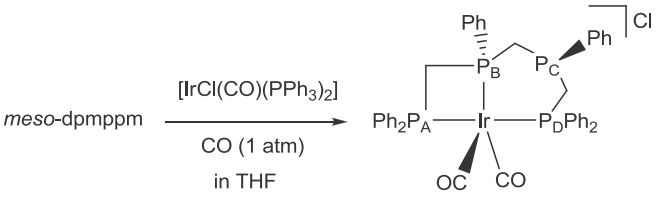

1

Scheme 2. Preparation of [Ir(*meso*-dpmppm−κ^3)(CO)$_2$]Cl (**1**).

2.2. Mononuclear Ir^{III} complexes with meso-dpmppm, [IrH(meso-dpmppm−κ^3)(CO)$_2$]X$_2$ (X = Cl (**2**), PF$_6$ (**2***)), [IrH(meso-dpmppm−κ^3)(RNC)$_2$](PF$_6$)$_2$ (R = Xyl (**3a**), Mes (**3b**), Cy (**3c**), ^{t}Bu (**3d**)), and [IrH(meso-dpmppm−κ^3)(MeCN)$_2$](PF$_6$)$_2$ (**3e**)

Complex **1** readily reacted with HCl in CH$_2$Cl$_2$ at room temperature to give [IrH(*meso*-dpmppm−κ^3)(CO)$_2$]Cl$_2$ (**2**) in 76% yield (Scheme 3), which was further converted into [IrH(*meso*-dpmppm−κ^3)(CO)$_2$](PF$_6$)$_2$ (**2***) by treatment with excess NH$_4$PF$_6$. Interestingly, complex **2*** was synthesized from reaction of **1** with NH$_4$PF$_6$ in a moderate yield (47%). Since reaction of **1** with KPF$_6$ did not afford **2*** at all, the source of the hydride should be NH_4^+ ion. By a similar procedure with mixing [IrCl(cod)]$_2$ (0.5 eq.), *meso*-dpmppm (1 eq.), RNC (2 eq.) in the presence of excess NH$_4$PF$_6$ in CH$_2$Cl$_2$, a series of hydride bisisocyanide Ir^{III} complexes, [IrH(*meso*-dpmppm−κ^3)(RNC)$_2$](PF$_6$)$_2$ (R = Xyl (**3a**), Mes (**3b**), Cy (**3c**), ^{t}Bu (**3d**)), were obtained in good yields (58−79%). Complexes **3** were barely generated from reaction of **2*** with 2 eq. of RNC in very low yields due to instability of **2***. The ^{31}P{^{1}H} NMR spectrum of **2** in CD$_2$Cl$_2$ showed the diagnostic spectral patterns for {Ir(*meso*-dpmppm−κ^3)} pincer unit at δ_{PA} −45.5 (dd, $J_{PP'}$ = 285, 57 Hz), δ_{PB} −53.4 (ddd, $J_{PP'}$ = 70, 57, 26 Hz), δ_{PC} −38.7 (dd, $J_{PP'}$ = 70, 42 Hz), and δ_{PD} −17.3 (ddd, $J_{PP'}$ = 285, 42, 26 Hz) (Fig. S5b), where *trans*-P_AP_D coupling constant (285 Hz) is definitely larger than that of **1** (174 Hz). The ^{1}H NMR spectrum of **2** displays a hydride peak at −15.67 ppm as a quartet due to coupling with three ^{31}P nuclei ($^2J_{PH}$ = 9 Hz) (Fig. S8a). In the IR spectrum, an intense ν_{CO} band was observed at 2068 cm^{-1} which is significantly high energy shifted from those of **1** owing to oxidation of the Ir center from +1 to +3. The ESI−MS spectrum showed a parent cation peak at *m*/*z* = 885.211 (*z* = 1) corresponding to {IrH(Cl)(dpmppm)(CO)}$^+$ (*m*/*z* = 885.111) (Fig. S10). The ^{31}P{^{1}H} NMR spectra of **3a-d** are almost identical independent of RNC (Fig. S6); e.g. that of **3a** showed the characteristic four resonances at δ_{PA} −51.8 (dd, $J_{PP'}$ = 262, 50 Hz), δ_{PB} −69.6 (ddd, $J_{PP'}$ = 62, 50, 21 Hz), δ_{PC} −40.6 (dd, $J_{PP'}$ = 62, 43 Hz), and δ_{PD} −20.6 (ddd, $J_{PP'}$ = 262, 43, 21 Hz) (Fig. S6a), with *trans*-P_AP_D coupling of 262 Hz which is almost same as that of **2** (285 Hz). In the ^{1}H NMR spectra (Fig. S8b), a quartet hydride peak ($^2J_{PH}$ = 14 Hz) was observed around −9.32 to −10.07 ppm, which is down field shifted by ca. 6 ppm from that of **2**. The ESI−MS spectra of **3a-d** in CH$_2$Cl$_2$ (Fig. S11) exhibited an intense monocation peak of {[IrH(dpmppm)(RNC)$_2$]PF$_6$}$^+$ at *m*/*z* = 1229.358 (**3a**), 1257.387 (**3b**), 1185.432 (**3c**), and 1133.426 (**3d**), and the IR spectrum exhibited two ν_{NC} peaks at around 2235−2181 cm^{-1}.

The detailed structure of **3a** was determined by X-ray diffraction analysis to consist of an octahedral Ir^{III} center coordinated by a *meso*-dpmppm ligand, two XylNC, and a hydride (Fig. 1 and Fig. S1, Table 1 and Table S3). The *meso*-dpmppm ligand coordinates to the Ir center with two outer (P1, P4) and one inner (P2) phosphorus atoms in an unsymmetric κ^3*PPP* pincer form as observed in [MCl(*meso*-dpmppm−κ^3)]X (M = Pt, Pd; X = Cl, PF$_6$) [48,61], where six- and four-membered chelate rings are fused, and the remaining inner P atom (P3) is uncoordinated (Ir1−P1 = 2.3682(7) Å, Ir1−P2 = 2.3092(7) Å, Ir1−P4 = 2.3536(8) Å). The six-membered ring takes a stable chair conformation and the phenyl group on P3 atom occupies an equatorial position. The P2−Ir1−P4 bite angles for six-membered ring is 95.52(2)°, and the P1−Ir1−P2 angles for four-membered ring is 71.04(2)°. The *trans* angle of P1−Ir1−P4 is 162.46(2)°. The bicyclic chelate ring system constrains three phenyl

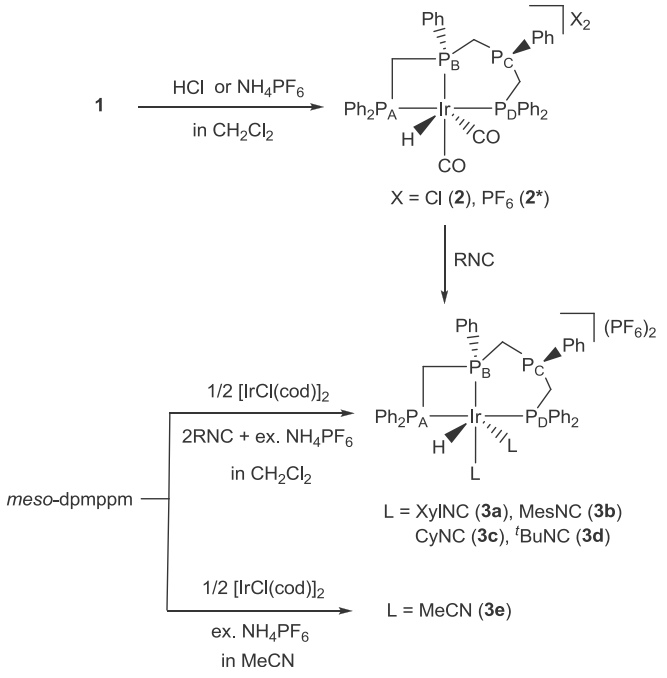

Scheme 3. Preparations of [IrH(*meso*-dpmppm−κ^3)(CO)]X$_2$ (X = Cl (**2**), PF$_6$ (**2***)), [IrH(*meso*-dpmppm−κ^3)(RNC)$_2$](PF$_6$)$_2$ (R = Xyl (**3a**), Mes (**3b**), Cy (**3c**), ^{t}Bu (**3d**)), and [IrH(*meso*-dpmppm−κ^3)(MeCN)$_2$](PF$_6$)$_2$ (**3e**).

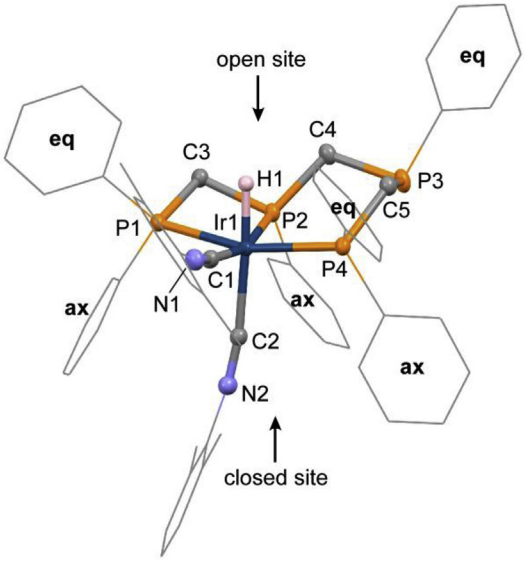

Fig. 1. Perspective view for the complex cation of [IrH(*meso*-dpmppm−κ^3)(XylNC)$_2$](PF$_6$)$_2$ (**3a**) with atomic numbering schemes. The thermal ellipsoids are drawn at the 40% probability level. The phenyl and xylyl groups are illustrated with wire models and C–H hydrogen atoms are omitted for clarity. **eq** indicates equatorially oriented phenyl groups of *meso*-dpmppm and **ax** indicates axially oriented ones. Ir (dark blue), P (orange), N (light blue), C (gray), and H (pink). (For interpretation of the references to color in this figure legend, the reader is referred to the Web version of this article.)

groups of P1, P2, and P4 atoms to axial direction (**ax**) with respect to the {Ir(*meso*-dpmppm−κ^3)} pincer plane (closed site), and the other three phenyl groups are in equatorial orientation (**eq**) on the other side of the plane (open site) (Fig. 1). The hydride was determined by difference Fourier syntheses at the axial open site with respect to the Ir(*PPP*) plane (Ir–H = 1.48(3) Å) and two isocyanides

Table 1
Structural Parameters of **3a**, **4**, **5a**, and **5b**.[a]

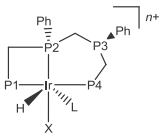

	3a	4	5a	5b
n	2	1	1	1
X	XylNC (C1)	H$^-$ (H41)	SiMe$_2$Ph$^-$	SiHPh$_2^-$
L	XylNC (C2)	CO (C1)	CO (C1)	CO
Ir–P1	2.3682(7)	2.3258(16)	2.3601(11)	2.3746(19)
Ir–P2	2.3092(7)	2.3399(18)	2.3862(11)	2.391(2)
Ir–P4	2.3536(8)	2.2939(17)	2.3303(11)	2.3315(19)
Ir–L	2.032(3) (C2)	1.936(5) (C1)	1.941(5) (C1)	1.965(10) (C1)
Ir–X	2.002(2) (C1)	1.52(9) (H41)	2.4527(12)	2.436(2)
Ir–H	1.48(3)	1.51(5) (H42)	1.50(5) (H52)	1.48 (H1)
P1–Ir–P2	71.04(2)	70.84(6)	69.39(3)	70.06(6)
P1–Ir–P4	162.46(2)	162.17(4)	157.52(4)	157.27(6)
P2–Ir–P4	95.52(2)	98.79(6)	94.63(3)	96.31(6)
P1–Ir–L	93.50(8)	100.9(2)	101.14(15)	98.2(2)
P2–Ir–L	98.93(8)	102.6(2)	101.41(15)	97.2(2)
P4–Ir–L	99.87(8)	95.5(2)	97.40(14)	101.6(2)
P1–Ir–X	99.54(9)	95(2)	94.00(4)	102.05(7)
P2–Ir–X	165.06(8)	163(2)	161.98(4)	171.39(4)
P4–Ir–X	91.09(9)	92(3)	99.16(4)	90.01(7)
L–Ir–X	93.08(12)	89(2)	88.31(15)	87.2(2)
P1–Ir–H	82.8(14)	74(3)	87(2)	88.5
P2–Ir–H	81.1(13)	80(3)	84(2)	94.0
P4–Ir–H	84.0(14)	90(3)	76(2)	74.0
L–Ir–H	176.1(15)	173(3)	171(2)	168.4
X–Ir–H	86.3(13)	87(4)	88(2)	82.1

[a] The atomic numbering schemes are shown in Figs. 1–3 and Figure S1–S4.

are attached at the other axial closed site (Ir1–C2 = 2.032(3) Å) and at equatorial position *trans* to P2 (Ir1–C1 = 2.002); the former bond distance is slightly longer than the latter value due presumably to strong *trans* influence of the hydride.

By the spectroscopic similarity between **2** and **3**, the structure of **2** is assumed to have an octahedral Ir^{III} geometry like **3a**, in which two isocyanide ligands are replaced by two carbonyl moieties. In the present reaction of **1** with HCl, an Ir^{III} complex formulated as [IrH(Cl)(*meso*-dpmppm−κ^3)(CO)]Cl was not obtained at all, although the square planar Ir^I pincer complex, [Ir(POCOP^{tBu})(CO)], underwent oxidative addition of HCl to give the chloride coordinated Ir^{III} complexes with H$^-$ and Cl$^-$ ligands in mutual *trans* positions [63].

When [IrCl(cod)]$_2$ (0.5 eq.) was treated with *meso*-dpmppm (1 eq.) and excess NH$_4$PF$_6$ in acetonitrile, an Ir^{III} hydride/acetonitrile complex, [IrH(*meso*-dpmppm−κ^3)(MeCN)$_2$](PF$_6$)$_2$ (**3e**), was obtained (Scheme 3). The ^{31}P{^{1}H} NMR spectra of **3e** showed the characteristic four resonances at δ_{PA} −42.1 (dd, $J_{PP'}$ = 325, 51 Hz), δ_{PB} −58.1 (ddd, $J_{PP'}$ = 67, 51, 20 Hz), δ_{PC} −39.5 (dd, $J_{PP'}$ = 67, 42 Hz), and δ_{PD} −11.4 (ddd, $J_{PP'}$ = 325, 42, 20 Hz) (Fig. S7a). The *trans*-P$_A$P$_D$ coupling constant (325 Hz) is appreciably larger than those of **2** (285 Hz) and **3a-d** (262–267 Hz). In the ^{1}H NMR spectrum (Fig. S8c), a quartet hydride peak ($^2J_{PH}$ = 13 Hz) was observed at −17.95 ppm which is significantly up-field shifted from the values of **2** (−15.67 ppm) and **3** (−9.32 to −10.07 ppm).

2.3. Reactions of **1** with H_2, formic acid, and hydrosilanes to form [Ir(H)$_2$(meso-dpmppm−κ^3)(CO)]Cl (**4**) and [IrH(SiR$_3$)(meso-dpmppm−κ^3)(CO)]Cl (R = Me$_2$Ph (**5a**), HPh$_2$ (**5b**))

Complex **1** was subject to oxidative addition of H$_2$ (1 atm) in CH$_2$Cl$_2$ at room temperature and afford an Ir^{III} dihydride complex,

[Ir(H)$_2$(*meso*-dpmppm−κ^3)(CO)]Cl (**4**), which was isolated as colorless single crystals in 39% yield (Scheme 4). The IR spectra showed a C≡O stretching band at 2005 cm^{-1} together with an Ir−H peak at 2106 cm^{-1}, and the ESI−MS spectrum in CH_2Cl_2 displayed a prominent peak at $m/z = 851.199$ ($z = 1$) corresponding to the complex cation of [Ir(H)$_2$(dpmppm)(CO)]$^+$ ($m/z = 851.151$) (Fig. S12). The ^{31}P{^{1}H} NMR spectrum of **4** in CD_2Cl_2 showed four resonances at δ_{PA} −45.4 (dd, $J_{PP'} = 267$, 38 Hz), δ_{PB} −62.6 (ddd, $J_{PP'} = 106$, 38, 21 Hz), δ_{PC} −35.2 (dd, $J_{PP'} = 106$, 45 Hz), and δ_{PD} −12.9 (ddd, $J_{PP'} = 267$, 45, 21 Hz) (Fig. S7b), which are similar to those of **2** except the up-filed shifted P_B signal due to large *trans* influence of the hydride. The ^{1}H NMR spectrum (Fig. S8d) exhibited two hydride peaks at −11.37 ppm as a doublet of doublets ($^2J_{PH} = 117$ Hz, 15 Hz) and at −9.13 ppm as a quartet ($^2J_{PH} = 15$ Hz), which are assignable to the hydrides at equatorial and axial positions, respectively, in regard to the Ir pincer plane and in agreement with the crystal structure described below.

The structure of **4** was determined by an X-ray analysis to have an Ir^{III} octahedral structure containing {Ir^{III}(*meso*-dpmppm−κ^3)} pincer unit; Ir1−P1 = 2.3258(16) Å, Ir1−P2 = 2.3399(18) Å, Ir1−P4 = 2.2939(17) Å, P1−Ir1−P2 = 70.84(6)°, P1−Ir1−P4 = 162.17(4)°, P2−Ir1−P4 = 98.79(6)° (Fig. 2 and Fig. S2, and Table 1 and Table S4). The other meridional sites are occupied by two hydride and one CO ligands; Ir1−C1 = 1.936(5) Å, Ir1−H41 = 1.52(9) Å, Ir1−H42 = 1.51(5) Å. The hydride positions were determined by DF syntheses. The Ir1−P2 bond length is elongated owing to *trans* influence of the hydride (H41) and is longer than those for the lateral P atoms (P1, P4). While it is well known that concerted oxidative addition of dihydrogen to d^8 Ir^I center is likely to afford kinetically preferred *cis*-dihydride complexes, isolated and characterized *cis*-dihydride carbonyl Ir^{III} complexes with pincer ligands have relatively been few [65–67] due to isomerization to thermodynamically stable *trans*-dihydride species and/or dissociation of dihydride as H_2 to regenerate Ir^I starting materials [68–71]. Milstein et al. reported that H_2 addition (1 atm, r.t.) to [Ir(PCP^{iPr})(CO)] (PCP^{iPr} = 1,3-[C$_6$H$_3$(CH$_2$P^{i}Pr$_2$)$_2$]$^-$) generated a *cis*-dihydride complex of [Ir(H)$_2$(PCP^{iPr})(CO)], which was converted to *trans*-isomer upon heating at 90 °C under pressurized H_2 [71]. Roddick et al. have also reported that [Ir(PCP^{CF3})(CO)] (PCP^{CF3} = 1,3-[C$_6$H$_3$(CH$_2$P(CF$_3$)$_2$)$_2$]$^-$) easily underwent addition of H_2 (1 atm,

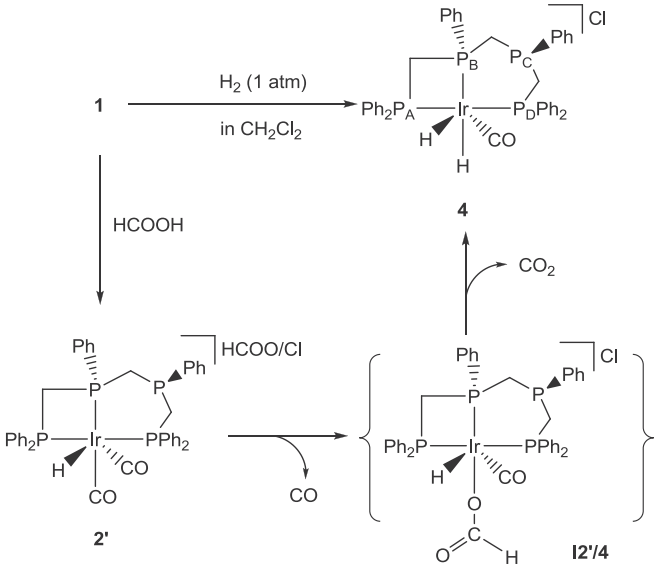

Scheme 4. Reactions of **1** with H_2 and HCOOH leading to [Ir(H)$_2$(*meso*-dpmppm−κ^3)(CO)]Cl (**4**).

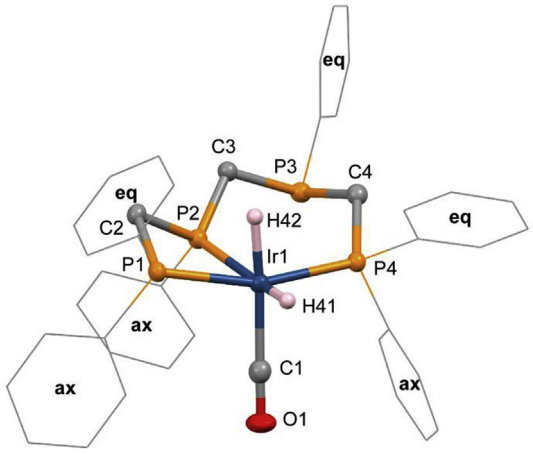

Fig. 2. Perspective view for the complex cation of [Ir(H)$_2$(*meso*-dpmppm−κ^3)(CO)]Cl (**4**) with atomic numbering schemes. The thermal ellipsoids are drawn at the 40% probability level. The phenyl groups are illustrated with wire models and C−H hydrogen atoms are omitted for clarity. **eq** indicates equatorially oriented phenyl groups of *meso*-dpmppm and **ax** indicates axially oriented ones. Ir (dark blue), P (orange), O (red), C (gray), and H (pink). (For interpretation of the references to color in this figure legend, the reader is referred to the Web version of this article.)

20 °C) to be converted exclusively into *trans*-[Ir(H)$_2$(PCP^{CF3})(CO)], VT ^{1}H NMR measurements of which revealed the presence of *mer*/*fac* isomerization of PCP^{CF3} as well as *cis*/*trans* isomerization of the dihydride Ir^{III} complex with *mer*-PCP^{CF3} scaffold [70]. In order to examine *cis*/*trans* and *mer*/*fac* isomerizations of **4**, variable temperature NMR measurements under N_2 were carried out, and demonstrated that the *cis*-dihydride isomer **4** was remarkably stable at −30 °C to 40 °C and would not be subject to any isomerization and decomposition, which might be ascribable to rigidity of the {Ir^{III}(*meso*-dpmppm−κ^3)} pincer unit. The *cis*-dihydride structure of **4** suggested that concerted oxidative addition of H_2 occurred at the open site of the pincer plane surrounded by equatorially directed phenyl groups, not at the closed site, to avoid steric repulsive interaction with phenyl groups of dpmppm ligand.

When complex **1** was treated with HCOOH in CH_2Cl_2 at room temperature, the monohydride complex [IrH(*meso*-dpmppm−κ^3)(CO)$_2$]X$_2$ (**2′**, X$_2$ = Cl/HCOO) was quantitatively generated in situ, and further work-up under reduced pressure unexpectedly gave birth to the dihydride complex **4** in a complete NMR yield (Scheme 4). Although the detailed mechanisms are not clear, the dihydrogen abstraction from formic acid may involve an formate complex, [IrH(HCOO)(*meso*-dpmppm−κ^3)(CO)]Cl (**I2′/4**), generated from dissociation of CO under reduced pressure, and β-hydrogen elimination of the formate to release CO_2 (Scheme 4).

Oxidative addition of hydrosilanes to **1** was examined since hydride silyl Ir^{III} species are recognized as very important intermediates in catalytic hydrosilylation of unsaturated organic compounds. Reactions of **1** with excess of Me$_2$PhSiH and Ph$_2$SiH$_2$ in CH_2Cl_2 proceeded at room temperature to afford [IrH(SiR$_3$)(*meso*-dpmppm−κ^3)(CO)]Cl (R$_3$ = Me$_2$Ph (**5a**), Ph$_2$H (**5b**)) in high yields based on ^{31}P{^{1}H} NMR spectra, which were successfully isolated as colorless crystals in yields of 28% (**5a**) and 62% (**5b**) (Scheme 5). The IR spectra showed ν_{CO} and ν_{IrH} peaks at 1985 cm^{-1} and 2099 cm^{-1} (**5a**) and 1993 cm^{-1} and 2103 cm^{-1} (**5b**), and the ESI−MS spectra in CH_2Cl_2 indicated a parent peak at $m/z = 985.330$ ($z = 1$) (**5a**) and 1033.284 ($z = 1$) (**5b**) corresponding to the complex cation of [IrH(SiR$_3$)(*meso*-dpmppm−κ^3)(CO)]$^+$ ($m/z = 985.206$ (**5a**), 1033.206 (**5b**)) (Fig. S13). The ^{31}P{^{1}H} NMR spectra of **5a**,**b** in CD_2Cl_2 presented four typical resonances of {Ir^{III}(*meso*-dpmppm−κ^3)} pincer unit at δ_{PA} −43.9 (dd, $J_{PP'} = 266$, 45 Hz), δ_{PB} −60.5 (ddd, $J_{PP'} = 92$, 45,

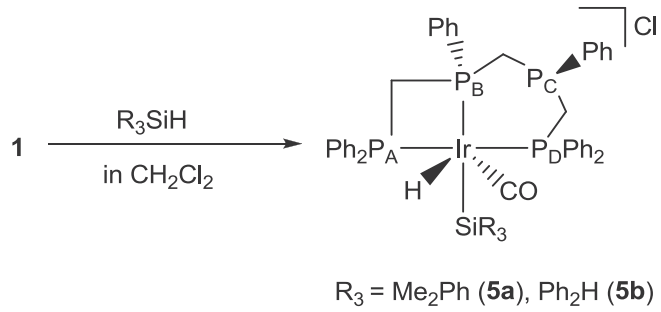

Scheme 5. Reactions of **1** with R_3SiH leading to [IrH(SiR_3)(*meso*-dpmppm−κ^3)(CO)]Cl (R_3 = Me_2Ph (**5a**), Ph_2H (**5b**)).

27 Hz), δ_{PC} −41.1 (dd, $J_{PP'}$ = 92, 51 Hz), and δ_{PD} −16.6 (ddd, $J_{PP'}$ = 266, 51, 27 Hz) for **5a** and at δ_{PA} −50.2 (dd, $J_{PP'}$ = 263, 46 Hz), δ_{PB} −61.6 (ddd, $J_{PP'}$ = 88, 46, 26 Hz), δ_{PC} −39.6 (dd, $J_{PP'}$ = 88, 50 Hz), and δ_{PD} −18.5 (ddd, $J_{PP'}$ = 263, 50, 26 Hz) for **5b** (Figs. S7c and d). The ^{1}H NMR spectra (Fig. S8e) exhibited a quartet hydride peak at −7.41 ppm ($^2J_{PH}$ = 18 Hz) (**5a**) and at −7.20 ppm ($^2J_{PH}$ = 15 Hz) (**5b**).

Complexes **5a** and **5b** were characterized by X-ray diffraction analyses (Fig. 3, Fig. S3 4 and Table 1, Table S5,6) to have Ir^{III} octahedral structures analogous to that of **4**, in which the equatorial hydride is replaced by a silyl group ($SiMe_2Ph$ (**5a**) and $SiHPh_2$ (**5b**)). The hydride and silyl H atoms were determined by difference Fourier syntheses. The Ir1−P2 bond lengths (2.3862(11) Å (**5a**), 2.391(2) Å (**5b**)) are appreciably longer than those of **4** (2.3399(18) Å) and **3a** (2.3092(7) Å) owing to stronger σ-donating ability of the silyl ligand. Whereas the Ir−Si bond lengths (2.4527(12) Å (**5a**), 2.436(2) Å (**5b**)) are noticeably longer than the reported values for other Ir^{III}–SiR_3 derivatives [72–74], the distances between the hydride and the Si atoms (2.832 Å (**5a**), 2.671 Å (**5b**)) clearly indicate no bonding interaction between them and consequently, **5a**,**b** could be recognized as classical hydride silyl Ir^{III} complexes. Steric

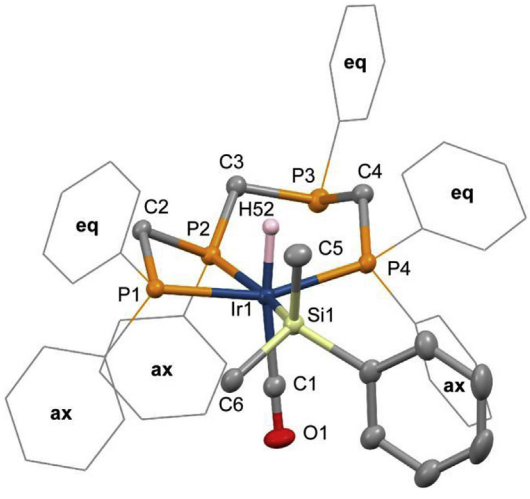

Fig. 3. Perspective view for the complex cation of [IrH($SiMe_2Ph$)(*meso*-dpmppm−κ^3)(CO)]Cl (**5a**) with atomic numbering schemes. The thermal ellipsoids are drawn at the 40% probability level. The phenyl groups of *meso*-dpmppm are illustrated with wire models and C−H hydrogen atoms are omitted for clarity. **eq** indicates equatorially oriented phenyl groups of *meso*-dpmppm and **ax** indicates axially oriented ones. Ir (dark blue), P (orange), Si (pale yellow), O (red), C (gray), and H (pink). (For interpretation of the references to color in this figure legend, the reader is referred to the Web version of this article.)

bulkiness of the silyl ligands leads to somewhat lager deformation from an octahedron in comparison with **4** (P1−Ir1−P4 = 157.52(4)° (**5a**), 157.27(6) ° (**5b**)). Noteworthy is that in spite of importance as intermediate species in various catalytic transformations of organosilanes, characterized hydride silyl Ir^{III} complexes with pincer ligands are very limited to only few examples, including [IrH(Cl)(-$SiEt_3$)(Xant(P^iPr_2)$_2$)] and [Ir(H)$_2$($SiClPh_2$)(Xant(P^iPr_2)$_2$)] (Xant(-P^iPr_2)$_2$ = 9,9-dimethyl-4,5-bis(diisopropylphosphino)xanthene) [72], [IrH(SiR_3)(PNP^{Ph})] (R = Ph, Et; PNP^{Ph} = [N(2-PPh_2-4-Me-C_6H_3)$_2$]$^-$) [73], [IrH(SiR_3)($POCOP^{tBu}$)] (R = Me_2Ph, Et_3; $POCOP^{tBu}$ = 2,6-[(OP^tBu_2)$_2$$C_6H_3$]$^-$) [74], the latter complexes involving η^2−Si−H σ coordination to the Ir^I center.

Substituents effects of hydrosilanes were examined by $^{31}P\{^1H\}$ NMR spectral changes using $MePh_2SiH$, Me_2PhSiH, and Et_3SiH, and the reactions with **1** completed after 20 min for $MePh_2SiH$, 1.5 h for Me_2PhSiH, and 1 d for Et_3SiH in CD_2Cl_2 at room temperature (Figs. S14 and S16a-c), the order of which is consistent with the known reactivity of silanes with Vaska type complexes and electronegative substituents accelerate oxidative addition of Si−H [75–77]. In the initial stage for reaction of **1** with Ph_2SiH_2 (after 15 min), the $^{31}P\{^1H\}$ NMR spectra disclosed the presence of an isomer **5b*** in a 0.8/1.0 ratio for **5b** (Figs. S15 and S16d), which disappeared after 1 d to indicate **5b** exclusively. Although the structure was not characterized, **5b*** is presumed to take an isomeric structure that possess another *trans*-H, CO form with the hydride in the closed site.

2.4. Addition of η^5−Cp*MCl_2 fragment onto the uncoordinate P atom of {Ir(*meso*-dpmppm−κ^3)} pincer unit

In order to examine allosteric influence of attaching {IrCp*Cl_2} fragment (Cp* = pentamethylcyclopentadienyl) onto the uncoordinate phosphine of {Ir^I(*meso*-dpmppm−κ^3)} pincer unit, which is assumed to take place conformational change of the six-membered chelate ring from a stable chair form to a sterically demanded twist boat one as observed for the {Pt^{II}(*meso*-dpmppm−κ^3)} complex [61], reactions of **1** with H_2, HCl, and Me_2PhSiH in the presence of [IrCp*Cl_2]$_2$ (0.5 eq.) were investigated by ^{1}H and $^{31}P\{^1H\}$ NMR and ESI mass spectroscopy.

The uncoordinate inner phosphine of **1** is readily reacted with [Cp*$IrCl_2$]$_2$ in CH_2Cl_2 at room temperature to give [Ir(μ−*meso*-dpmppm−κ^3,κ^1)(η^5−Cp*$IrCl_2$)(CO)$_2$]Cl (**1**·Cp*$IrCl_2$) (Scheme 6). The $^{31}P\{^1H\}$ NMR spectrum of the reaction mixture (Fig. S17a) exhibited a predominant existence of **1**·Cp*$IrCl_2$ by four characteristic resonances at δ −88.2 (P_B), −68.2 (P_A), −28.2 (P_D) and 2.1 (P_C) with $^2J_{PAPB}$ = 73 Hz, $^2J_{PAPD}$ = 231 Hz, $^2J_{PBPC}$ = 10 Hz, $^2J_{PBPD}$ = 34 Hz, and $^2J_{PCPD}$ = 26 Hz, where the peak of P_C considerably down field shifted from that of **1** (−33.6 ppm) and $^2J_{PP'}$ coupling constants for P_C appreciably decreased from those of **1** ($^2J_{PBPC}$ = 87 Hz, $^2J_{PCPD}$ = 73 Hz), due to coordination of P_C to {IrCp*Cl_2} unit. The methyl protons of Cp* are observed at 1.46 ppm as a doublet coupling to P_C. These spectral features are also observed for [PtCl(μ−*meso*-dpmppm−κ^3,κ^1)(η^5−Cp*$IrCl_2$)]PF_6 [61]. The ESI−MS spectrum of the reaction mixture exhibited a prominent monocation peak at *m*/*z* = 1247.329 (*z* = 1) corresponding to {Ir(dpmppm)(IrCp*Cl_2)(CO)}$^+$ (*m*/*z* = 1247.151) (Fig. S19a). The adduct of **1**·Cp*$IrCl_2$ easily underwent oxidative addition of H_2 (1 atm) at room temperature to result in [Ir(H)$_2$(μ−*meso*-dpmppm−κ^3)(η^5−Cp*$IrCl_2$)(CO)]Cl (**4**·Cp*$IrCl_2$) (Scheme 6). The $^{31}P\{^1H\}$ NMR spectrum of the reaction mixture (Fig. S17c) revealed an exclusive formation of **4**·Cp*$IrCl_2$ at δ −73.2 (P_B), −51.7 (P_A), −19.3 (P_D) and 1.8 (P_C) with $^2J_{PAPB}$ = 25 Hz, $^2J_{PAPD}$ = 262 Hz, $^2J_{PBPC}$ = 16 Hz, $^2J_{PBPD}$ = 21 Hz, and $^2J_{PCPD}$ = 26 Hz. The peculiar spectral changes for P_C gave an account of its ligation to the IrCp*Cl_2 unit. In the ^{1}H NMR spectrum (Fig. S18b), two hydride peaks were

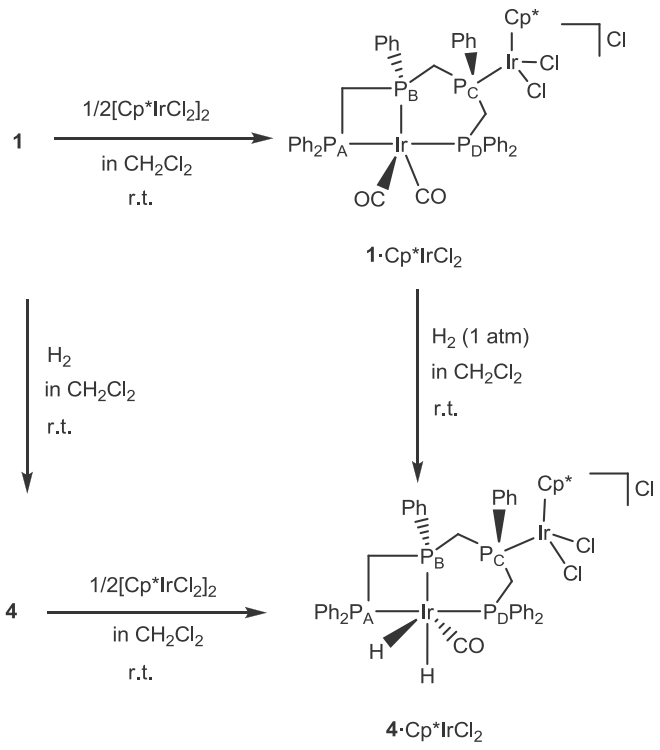

Scheme 6. Reactions of **1** and **4** with $[IrCp^*Cl_2]_2$ (0.5 eq.) leading to **1**·$IrCp^*Cl_2$ and **4**·$IrCp^*Cl_2$, and that of **1**·$IrCp^*Cl_2$ with H_2 (1 atm) to give **4**·$IrCp^*Cl_2$.

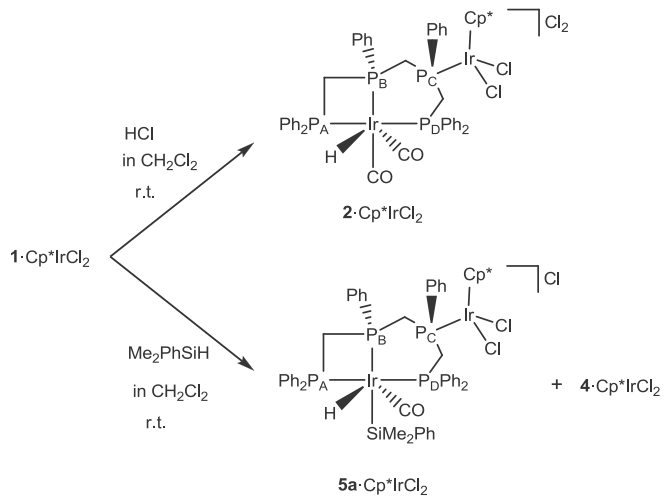

Scheme 7. Reactions of **1**·$IrCp^*Cl_2$ with HCl and Me_2PhSiH resulting in **2**·$IrCp^*Cl_2$ and in a 1:2 mixture of **5a**·$IrCp^*Cl_2$ and **4**·$IrCp^*Cl_2$, respectively.

observed at −9.34 ppm as a quartet ($^2J_{PH}$ = 16 Hz) and −11.59 ppm as a broad doublet ($^2J_{PH}$ = 118 Hz), which were quite similar to those of **4** at −9.13 ($^2J_{PH}$ = 15 Hz) and −11.37 ($^2J_{PH}$ = 117, 15 Hz), and the Cp* methyl signal was observed at 1.36 ppm as a doublet ($^2J_{PH}$ = 16 Hz). The ESI−MS spectrum of the reaction mixture exhibited an intense predominant peak at m/z = 1249.345 (z = 1) for the complex cation of $[Ir(H)_2(dpmppm)(IrCp^*Cl_2)(CO)]^+$ (m/z = 1249.166) (Fig. S19b). Complex **4** was also transformed by treating with $[Cp^*IrCl_2]_2$ to **4**·Cp^*IrCl_2 quantitatively. These results demonstrated that concerted oxidative addition of H_2 to **1** was no longer interrupted by the structural switch induced from an attachment of $\{IrCp^*Cl_2\}$ unit to the uncoordinate Pc atom. Noted that **4**·Cp^*IrCl_2 would not react with further 0.5 equiv of $[IrCp^*Cl_2]_2$. Similarly, a complete conversion of **1**·Cp^*IrCl_2 to $[IrH(\mu\text{-}meso\text{-}dpmppm\text{-}\kappa^3)(\eta^5\text{-}Cp^*IrCl_2)(CO)_2]Cl_2$ (**2**·Cp^*IrCl_2) was established by reacting with HCl (Scheme 7, Figs. S17b, S18a, and S19c).

In contrast, reaction of **1**·Cp^*IrCl_2 with bulky Me_2PhSiH (3 eq.) resulted in a disproportionation mixture of $[IrH(Me_2PhSi)(\mu\text{-}meso\text{-}dpmppm\text{-}\kappa^3)(\eta^5\text{-}Cp^*IrCl_2)(CO)]Cl$ (**5a**·Cp^*IrCl_2) and **4**·Cp^*IrCl_2 in a 1:2 ratio together with small amounts of many unidentified byproducts (Scheme 7). The ^1H NMR spectrum of the reaction mixture for the hydride region (Fig. S18c) displayed three resonances at −8.32 ppm as a quartet ($^2J_{PH}$ = 15 Hz), −9.34 ppm as a quartet ($^2J_{PH}$ = 16 Hz), and −11.59 ppm as a broad double ($^2J_{PH}$ = 118 Hz) in ca. 1:2:2 ratio, the latter major two being assignable to a *cis*-dihydride Ir^{III} species of **4**·Cp^*IrCl_2 and the former minor one corresponding to a monohydride at an axial position vs $\{Ir(meso\text{-}dpmppm\text{-}\kappa^3)\}$ pincer plane. In the $^{31}P\{^1H\}$ NMR spectrum (Fig. S17d), two sets of diagnostic four resonances were observed as indicated with $P_{A,B,C,D}$ and $P_{A',B',C',D'}$; and the former major set is corresponding to **4**·Cp^*IrCl_2 and the latter minor set should be assignable to $[IrH(Me_2PhSi)(\eta^5\text{-}Cp^*IrCl_2)(\mu\text{-}meso\text{-}dpmppm\text{-}\kappa^3)(CO)]Cl$ (**5a**·Cp^*IrCl_2), on the basis of the NMR spectral features, δ −76.4 ($P_{B'}$), −54.2 ($P_{A'}$), −22.4 ($P_{D'}$) and −4.1 ($P_{C'}$) with $^2J_{PA'PB'}$ = 35 Hz, $^2J_{PA'PD'}$ = 265 Hz, $^2J_{PB'PC'}$ = 11 Hz, $^2J_{PB'PD'}$ = 21 Hz, and $^2J_{PC'PD'}$ = 29 Hz, and the ESI−MS peak for $[IrH(Me_2PhSi)(Cp^*IrCl_2)(meso\text{-}dpmppm)(CO)]^+$ at m/z = 1383.252 (z = 1) (Fig. S19d). Although formation mechanisms for **4**·Cp^*IrCl_2 are unknown, the allosteric influence by attaching Cp^*IrCl_2 unit on the uncoordinate phosphine of the $\{Ir(meso\text{-}dpmppm\text{-}\kappa^3)\}$ unsymmetric pincer unit in **1** definitely unstabilized the oxidative addition product of bulky Me_2PhSiH.

3. Conclusion

In the present study, a series of Ir^{III} hydride complexes with *meso*-dpmppm, $[IrH(meso\text{-}dpmppm\text{-}\kappa^3)(CO)_2]X_2$ (X = Cl (**2**), PF_6 (**2***)), $[IrH(meso\text{-}dpmppm\text{-}\kappa^3)(RNC)_2](PF_6)_2$ (R = Xyl (**3a**), Mes (**3b**), Cy (**3c**), ^{t}Bu (**3d**)), $[Ir(H)_2(meso\text{-}dpmppm\text{-}\kappa^3)(CO)]Cl$ (**4**), and $[IrH(SiR_3)(meso\text{-}dpmppm\text{-}\kappa^3)(CO)]Cl$ (R_3 = Me_2Ph (**5a**), Ph_2H (**5b**)) were synthesized by oxidative additions of HX, H_2, HCOOH, and R_3SiH, (for **2**, **4**, **5**) to $[Ir^I(meso\text{-}dpmppm\text{-}\kappa^3)(CO)_2]Cl$ (**1**) and reactions of $[IrCl(cod)]_2$ with *meso*-dpmppm and RNC in the presence of NH_4PF_6 (for **3**). The tetraphosphine *meso*-dpmppm acts as an unsymmetric pincer ligand in meridional κ^3*PPP*−fashion, and rigidly coordinates to the Ir center with two outer and one inner phosphorus atoms to form fused six- and four-membered chelate rings with an uncoordinate inner phosphine unit. The structural features of the isolated complexes suggested that oxidative additions of H^+, H_2, and R_3SiH occurred at the axial open site surrounded by equatorially oriented phenyl groups of *meso*-dpmppm. The uncoordinate inner phosphine of **1** is readily reacted with $[Cp^*IrCl_2]_2$ to give an adduct of **1**·Cp^*IrCl_2, which was further transformed by oxidative addition of H_2 and HCl to **4**·Cp^*IrCl_2 and **2**·Cp^*IrCl_2, respectively, and however addition of bulky Me_2PhSiH resulted in a disproportionation mixture of **5a**·Cp^*IrCl_2 and **4**·Cp^*IrCl_2. The allosteric influence of conformational switch by attaching Cp^*IrCl_2 fragment on the uncoordinate phosphine unstabilized the oxidative addition product of bulky organosilanes but not for dihydrogen and HCl reactions. The present results could provide useful information as generally postulated key intermediate species to develop functional catalytic systems by utilizing unsymmetric pincer ligands.

4. Experimental

4.1. General

All preparative procedures were carried out under nitrogen atmosphere using standard Schlenk techniques. All chemicals (highest purity available) were purchased from Wako Pure Chemical Industries, Ltd. Reagent grade solvents were dried by the standard procedures and were freshly distilled prior to their use. Compounds *meso*-dpmpppm [44], $[IrCl(cod)]_2$ [78], $[IrCl(CO)(PPh_3)_2]$ [79], and $[Cp^*MCl_2]_2$ (M = Ir, Rh) [80] were prepared by the methods described in the literature. ^1H and $^1H\{^{31}P\}$ NMR spectra were recorded on a Bruker AV-300N instrument (300 MHz) and the frequencies were referenced to the residual resonances of the deuterated solvent. $^{31}P\{^1H\}$ NMR spectra were recorded on the same instrument at 121 MHz with chemical shifts being calibrated to 85% H_3PO_4 as an external reference. The assignments of ^{31}P NMR, P_A, P_B, P_C, and P_D are shown in Figs. S5–S7. IR spectra of solid samples as KBr disks were recorded on a JASCO FT/IR-410 spectrophotometer at ambient temperature. ESI–TOF mass spectra were recorded on a JEOL JMS-T100LC in a positive detection mode in the range of *m/z* 100–3000, equipped with an ion spray interface. The sprayer was held at a potential of +2.0 kV, and the compressed N_2 was employed to assist liquid nebulization.

4.2. Preparation of [Ir(meso-dpmpppm-κ^3)(CO)$_2$]Cl (**1**)

Under CO (1 atm) atmosphere, to a THF solution (1 mL) containing *meso*-dpmpppm (36 mg, 57 μmol) was added $[IrCl(CO)(PPh_3)_2]$ (45 mg, 57 μmol) and THF (2 mL). The mixture was stirred at room temperature for 30 min under stream of CO, and then the mixture was stirred under CO atmosphere overnight to deposit a white powder of **1**, which was separated by filtration, washed with diethyl ether, and dried under nitrogen (49 mg, 94% vs dpmpppm). Anal. Calc. for $C_{41}H_{36}O_2P_4ClIr$ (**1** (912.288)): C, 53.98; H, 3.98. Found: C, 54.05; H, 4.05. IR (KBr): ν 2004 (s, CO), 1973 (s, CO), 1435 (s), 1096 (m), 1059 (m), 836 (m), 744 (m), 693 (m), 513 (m), 495 (m) cm^{-1}.$^1H\{^{31}P\}$ NMR (CD_2Cl_2): δ 3.03 (d, 1H, C*H*$_2$), 3.14 (d, 1H, C*H*$_2$), 3.89 (d, 1H, C*H*$_2$), 4.54 (d, 1H, C*H*$_2$), 5.30 (d, 1H, C*H*$_2$), 6.68 (d, 1H, C*H*$_2$), 7.28–7.90 (m, 30H, Ar*H*). $^{31}P\{^1H\}$ NMR (CD_2Cl_2): δ −78.4 (ddd, 1P (P_B), $J_{PP'}$ = 87, 80, 29 Hz), −62.2 (dd, 1P (P_A), $J_{PP'}$ = 174, 80 Hz), −33.6 (dd, 1P (P_C), $J_{PP'}$ = 87, 73 Hz), −17.3 (ddd, 1P (P_D), $J_{PP'}$ = 174, 73, 29 Hz). ESI–MS (CH_2Cl_2): *m/z* 849.226 (*z*1, {Ir(dpmpppm)(CO)}$^+$ (849.135)).

4.3. Preparations of [Ir(H)(meso-dpmpppm-κ^3)(CO)$_2$]X$_2$ (X = Cl (**2**), PF$_6$ (**2***))

To a dichloromethane solution (8 mL) containing **1** (76 mg, 83 μmol) was added a methanolic solution of HCl (135 μL, 250 μmol), and the mixture was stirred at room temperature overnight. Then the solvent was removed under reduced pressure, and the residue was extracted with 7 mL of dichloromethane. The extract was passed through a membrane filter and was concentrated to ca. 2 mL, and diethyl ether (40 mL) was carefully added to give a white powder of **2**, which was separated by filtration, washed with diethyl ether, and dried under vacuum (60 mg, 76%). Anal. Calc. for $C_{41.5}H_{38}O_2P_4Cl_3Ir$ (**2**·0.5CH_2Cl_2 (991.216)): C, 50.29; H, 3.86. Found: C, 49.90; H, 4.03. IR (KBr): ν 2068 (s, CO), 1484 (m), 1435 (s), 1365 (m), 1102 (s), 1059 (m), 999 (m), 836 (m), 745 (s), 711 (s), 691 (s), 520 (s) cm^{-1}.$^1H\{^{31}P\}$ NMR (CD_2Cl_2): δ −15.67 (s, 1H, Ir*H*), 2.67 (d, 1H, C*H*$_2$), 3.07 (d, 1H, C*H*$_2$), 3.87 (d, 1H, C*H*$_2$), 4.01 (d, 1H, C*H*$_2$), 5.20 (d, 1H, C*H*$_2$), 6.06 (d, 1H, C*H*$_2$), 7.15–7.97 (m, 30H, Ar*H*). $^{31}P\{^1H\}$ NMR (CD_2Cl_2): δ −53.4 (ddd, 1P (P_B), $J_{PP'}$ = 70, 57, 26 Hz), −45.5 (dd, 1P (P_A), $J_{PP'}$ = 285, 57 Hz), −38.7 (dd, 1P (P_C), $J_{PP'}$ = 70, 42 Hz), −17.3 (ddd, 1P (P_D), $J_{PP'}$ = 285, 42, 26 Hz). ESI–MS (CH_2Cl_2): *m/z* 857.219 (*z*1, {IrH(dpmpppm)Cl}$^+$ (857.116)), *m/z* 885.211 (*z*1, {IrH(dpmpppm)(CO)Cl}$^+$ (885.111)).

To a dichloromethane solution (7 mL) containing **1** (35 mg, 38 μmol) was added NH_4PF_6 (13.8 mg, 85 μmol), and the mixture was stirred at room temperature overnight. The solvent was removed under reduced pressure, and the residue was extracted with 5 mL of dichloromethane. The extract was passed through a membrane filter and was concentrated to ca. 3 mL, and diethyl ether (3 mL) was carefully added, which was allowed to stand in refrigerator to afford an off-white powder of **2***. The product was separated by filtration, washed with diethyl ether, and dried under vacuum (21 mg, 47%). Anal. Calc. for $C_{41}H_{37}O_2F_{12}P_6Ir$ (**2*** (1167.772)): C, 42.17; H, 3.19. Found: C, 45.71; H, 3.54. Due to some contaminations, satisfactory analytical data was not obtained. IR (KBr): ν 2075 (s, CO), 2003 (s, CO), 1485 (m), 1437 (s), 1100 (m), 999 (m), 840 (s), 711 (m), 693 (m), 557 (m) cm^{-1}.$^1H\{^{31}P\}$ NMR (CD_2Cl_2): δ −15.57 (s, 1H, Ir*H*), 2.48 (d, 1H, C*H*$_2$), 2.68 (d, 1H, C*H*$_2$), 3.90 (d, 1H, C*H*$_2$), 4.06 (d, 1H, C*H*$_2$), 5.03 (d, 1H, C*H*$_2$), 5.34 (d, 1H, C*H*$_2$), 6.72–8.03 (m, 30H, Ar*H*). $^{31}P\{^1H\}$ NMR (CD_2Cl_2): δ −144.4 (sep, 2P (PF_6), J_{PF} = 712 Hz), −53.9 (ddd, 1P (P_B), $J_{PP'}$ = 70, 57, 26 Hz), −45.9 (dd, 1P (P_A), $J_{PP'}$ = 286, 57 Hz), −38.9 (dd, 1P (P_C), $J_{PP'}$ = 70, 43 Hz), −17.2 (ddd, 1P (P_D), $J_{PP'}$ = 286, 43, 26 Hz). ESI–MS (CH_2Cl_2): *m/z* 885.169 (*z*1, {IrH(dpmpppm)(CO)Cl}$^+$ (885.111)).

4.4. Preparations of [Ir(H)(meso-dpmpppm-κ^3)(RNC)$_2$](PF$_6$)$_2$ (R = Xyl (**3a**), Mes (**3b**), CyCN (**3c**), ^{t}Bu (**3d**))and [Ir(H)(dpmpppm−κ^3)(MeCN)$_2$](PF$_6$)$_2$ (**3e**)

For **3a**: To a dichloromethane solution (7 mL) containing *meso*-dpmpppm (51 mg, 82 μmol) were added $[IrCl(cod)]_2$ (28 mg, 42 μmol), NH_4PF_6 (57 mg, 0.35 mmol), and XylNC (47 mg, 0.36 mmol) successively over 2 h at room temperature, and the mixture was stirred overnight. The solvent was removed under reduced pressure to dryness, and the residue was washed with diethyl ether and extracted with dichloromethane (5 mL). The extract was passed through a membrane filter and was concentrated to ca. 0.5 mL, and diethyl ether (40 mL) was carefully added to give a white powder of **3a**, which was separated by filtration, washed with diethyl ether, and dried under vacuum (89 mg, 79%). Anal. Calc. for $C_{57}H_{55}N_2F_{12}P_6Ir$ (**3a** (1374.100)): C, 49.82; H, 4.03; N, 2.04. Found: C, 49.76; H, 3.77; N, 1.92. IR (KBr): ν 2208 (s, C≡N), 2189 (s, C≡N), 1477 (m), 1437 (s), 1376 (m), 1098 (s), 1000 (m), 842 (s), 743 (m), 711 (m), 691 (m), 557 (s) cm^{-1}.$^1H\{^{31}P\}$ NMR (CD_2Cl_2): δ −9.32 (s, 1H, Ir*H*), 1.58 (s, 6H, *o*-Me), 1.70 (s, 6H, *o*-Me), 3.04 (d, 1H, C*H*$_2$), 3.25 (d, 1H, C*H*$_2$), 3.61 (d, 1H, C*H*$_2$), 3.66 (d, 1H, C*H*$_2$), 4.84 (d, 1H, C*H*$_2$), 6.04 (d, 1H, C*H*$_2$), 6.98–7.91 (m, 36H, Ar*H*). $^{31}P\{^1H\}$ NMR (CD_2Cl_2): δ −144.6 (sep, 2P (PF_6), J_{PF} = 709 Hz), −69.6 (ddd, 1P (P_B), $J_{PP'}$ = 62, 50, 21 Hz), −51.8 (dd, 1P (P_A), $J_{PP'}$ = 262, 50 Hz), −40.6 (dd, 1P (P_C), $J_{PP'}$ = 62, 43 Hz), −20.6 (ddd, 1P (P_D), $J_{PP'}$ = 262, 43, 21 Hz). ESI–MS (CH_2Cl_2): *m/z* 1229.358 (*z*1, {[Ir(H)(dpmpppm)(XylNC)$_2$]PF_6}$^+$ (1229.259)). Recrystallization of **3a** from an acetonitrile/diethyl ether mixed solvent afforded prismatic colorless crystals of **3a**·2CH_3CN which were suitable for X-ray diffraction analysis.

For **3b**: By a procedure similar to that of **3a**, using MesNC instead of XylNC, **3b** was obtained in 58% yield. Anal. Calc. for $C_{59.5}H_{60}N_2F_{12}P_6ClIr$ (**3b**·0.5CH_2Cl_2 (1444.620)): C, 49.47; H, 4.19; N, 1.94. Found: C, 49.36; H, 3.89; N, 1.85. IR (KBr): ν 2197 (s, C≡N), 2181 (s, C≡N), 1484 (m), 1437 (s), 1381 (m), 1312 (m), 1268 (m), 1193 (m), 1098 (s), 1044 (m), 1000 (m), 837 (s), 740 (m), 693 (m), 557 (s) cm^{-1}.$^1H\{^{31}P\}$ NMR (CD_2Cl_2): δ −10.00 (s, 1H, Ir*H*), 1.44 (s, 6H, *o*-Me), 1.63 (s, 6H, *o*-Me), 2.24 (s, 3H, *p*-Me), 2.28 (s, 3H, *p*-Me), 3.00 (d, 1H, C*H*$_2$), 3.20 (d, 1H, C*H*$_2$), 3.57 (d, 1H, C*H*$_2$), 3.61 (d, 1H, C*H*$_2$), 4.80 (d, 1H, C*H*$_2$), 6.00 (d, 1H, C*H*$_2$), 6.78–7.89 (m, 34H, Ar*H*). $^{31}P\{^1H\}$ NMR (CD_2Cl_2): δ −144.3 (sep, 2P (PF_6), J_{PF} = 709 Hz), −69.3 (ddd, 1P

(P_B), $J_{PP'}$ = 68, 50, 21 Hz), −51.6 (dd, 1P (P_A), $J_{PP'}$ = 264, 50 Hz), −40.5 (dd, 1P (P_C), $J_{PP'}$ = 68, 48 Hz), −20.4 (ddd, 1P (P_D), $J_{PP'}$ = 264, 48, 21 Hz). ESI−MS (CH_2Cl_2): *m/z* 1257.387 (*z*1, {[Ir(H)(dpmppm)(-MesNC)$_2$]PF_6}$^+$ (1257.291)).

For **3c**: By a procedure similar to that of **3a**, using CyNC instead of XylNC, **3c** was obtained in 63% yield. Anal. Calc. for $C_{53.5}H_{60}N_2F_{12}P_6ClIr$ (**3c**·0.5CH_2Cl_2 (1372.556)): C, 46.82; H, 4.41; N, 2.04. Found: C, 46.68; H, 4.14; N, 2.00. IR (KBr): ν 2235 (s, C≡N), 2219 (s, C≡N), 1485 (m), 1437 (s), 1326 (m), 1314 (m), 1267 (m), 1110 (m), 1096 (m), 1000 (w), 839 (s), 745 (m), 693 (m), 557 (s), 493 (m) cm^{-1}.^{1}H{^{31}P} NMR (CD_2Cl_2): δ −10.07 (s, 1H, Ir*H*), 0.38−1.44 (br m, 20H, C*H*$_2$ (Cy)), 2.95 (d, 1H, C*H*$_2$), 3.17 (d, 1H, C*H*$_2$), 3.17 (d, 1H, C*H*$_2$), 3.36 (d, 1H, C*H*$_2$), 3.36 (d, 1H, C*H*$_2$), 3.54 (br t, 1H, C*H* (Cy)), 3.75 (br m, 1H, C*H* (Cy)), 5.98 (d, 1H, C*H*$_2$), 7.31−7.81 (m, 30H, Ar*H*). ^{31}P{^{1}H} NMR (CD_2Cl_2): δ −144.4 (sep, 2P (PF_6), J_{PF} = 709 Hz), −67.9 (ddd, 1P (P_B), $J_{PP'}$ = 66, 50, 21 Hz), −49.3 (dd, 1P (P_A), $J_{PP'}$ = 267, 50 Hz), −38.2 (dd, 1P (P_C), $J_{PP'}$ = 66, 44 Hz), −19.1 (ddd, 1P (P_D), $J_{PP'}$ = 267, 44, 21 Hz). ESI−MS (CH_2Cl_2): *m/z* 1185.432 (*z*1, {[Ir(H)(dpmppm)(CyNC)$_2$]PF_6}$^+$ (1185.290)).

For **3d**: By a procedure similar to that of **3a**, using ^{t}BuNC instead of XylNC, **3d** was obtained in 75% yield. Anal. Calc. for $C_{49}H_{55}N_2F_{12}P_6Ir$ (**3d** (1278.015)): C, 46.05; H, 4.34; N, 2.19. Found: C, 45.76; H, 4.24; N, 2.38. Due to unidentified contamination, satisfactory analytical data was not obtained. IR (KBr): ν 2224 (s, C≡N), 2210 (s, C≡N), 1485 (m), 1437 (s), 1373 (m), 1312 (m), 1236 (m), 1191 (s), 1104 (s), 1084 (m), 1058 (m), 999 (w), 881 (m), 743 (s), 711 (m), 694 (m), 482 (m) cm^{-1}.^{1}H{^{31}P} NMR (CD_2Cl_2): δ −10.00 (s, 1H, Ir*H*), 0.87 (s, 9H, C*H*$_3$ (^{t}Bu)), 0.97 (s, 9H, C*H*$_3$ (^{t}Bu)), 2.96 (d, 1H, C*H*$_2$), 3.13 (d, 1H, C*H*$_2$), 3.32 (d, 1H, C*H*$_2$), 3.42 (d, 1H, C*H*$_2$), 4.68 (d, 1H, C*H*$_2$), 6.04 (d, 1H, C*H*$_2$), 7.39−7.92 (m, 30H, Ar*H*). ^{31}P{^{1}H} NMR (CD_2Cl_2): δ −144.6 (sep, 2P (PF_6), J_{PF} = 709 Hz), −67.3 (ddd, 1P (P_B), $J_{PP'}$ = 70, 50, 21 Hz), −49.2 (dd, 1P (P_A), $J_{PP'}$ = 265, 50 Hz), −40.2 (dd, 1P (P_C), $J_{PP'}$ = 70, 48 Hz), −20.8 (ddd, 1P (P_D), $J_{PP'}$ = 265, 48, 21 Hz). ESI−MS (CH_2Cl_2): *m/z* 1133.426 (*z*1, {[Ir(H)(dpmppm)(^{t}BuNC)$_2$]PF_6}$^+$ (1133.259)).

For **3e**: To an acetonitrile solution (7 mL) containing *meso*-dpmppm (56 mg, 89 μmol) were added [IrCl(cod)]$_2$ (30 mg, 45 μmol) and NH_4PF_6 (66 mg, 0.41 mmol) successively over 20 min at room temperature, and the mixture was stirred overnight. The solvent was removed under reduced pressure to dryness, and the residue was washed with diethyl ether and extracted with acetonitrile (7 mL). The extract was passed through a membrane filter and was concentrated to ca. 0.5 mL, and diethyl ether (40 mL) was carefully added to give a pale yellow powder of **3e**, which was separated by filtration, washed with diethyl ether, and dried under vacuum (87 mg, 81%). Contamination of inorganic salts prevented from obtaining satisfactory analytical data. IR (KBr): ν 1486 (m), 1437 (s), 1403 (m), 1315 (m), 1191 (m), 1163 (m), 1101 (s), 1026 (m), 1000 (m), 839 (s), 742 (m), 710 (s), 693 (s), 557 (s), 496 (m) cm^{-1}.^{1}H {^{31}P} NMR (CD_3CN): δ −17.95 (s, 1H, Ir*H*), 2.86 (d, 1H, C*H*$_2$), 3.09 (m, 2H, C*H*$_2$), 3.38 (d, 1H, C*H*$_2$), 4.20 (d, 1H, C*H*$_2$), 5.85 (d, 1H, C*H*$_2$), 7.10−8.07 (m, 30H, Ar*H*). ^{31}P{^{1}H} NMR (CD_3CN): δ −144.3 (sep, 2P (PF_6), J_{PF} = 704 Hz), −58.1 (ddd, 1P (P_B), $J_{PP'}$ = 67, 51, 20 Hz), −42.1 (dd, 1P (P_A), $J_{PP'}$ = 325, 51 Hz), −39.5 (dd, 1P (P_C), $J_{PP'}$ = 67, 42 Hz), −11.4 (ddd, 1P (P_D), $J_{PP'}$ = 325, 42, 20 Hz).

4.5. Preparation of [Ir(H)$_2$(meso-dpmppm-κ^3)(CO)]Cl (**4**)

<Method 1> Stream of H_2 (1 atm) was introduced into a dichloromethane solution (10 mL) containing **1** (68 mg, 75 μmol) for 10 min, and the mixture was stirred at room temperature for 3 h under H_2 atmosphere (1 atm). Then, the solution was concentrated to ca. 7 mL under reduced pressure, and diethyl ether (2.5 mL) was carefully added to the solution, which was allowed to stand in refrigerator to afford colorless crystals of **4**. They were separated by filtration, washed with diethyl ether, and dried under vacuum (26 mg, 39%). <Method 2> To a dichloromethane solution (5 mL) containing **1** (51 mg, 56 μmol) was added formic acid (6.5 μL, 171 μmol) and CH_2Cl_2 (2.5 mL), and the mixture was stirred at room temperature overnight. The solvent was removed under reduced pressure, and the residue was washed with Et_2O, and extracted with CH_2Cl_2 (7 mL). The extract was passed through a membrane filter and was concentrated to ca. 5 mL, to which diethyl ether (4 mL) was carefully added to give colorless crystals of **4** (24 mg, 49%). Anal. Calc. for $C_{40.25}H_{38.5}OP_4Cl_{1.5}Ir$ (**4**·0.25CH_2Cl_2 (907.527)): C, 53.27; H, 4.28. Found: C, 53.50; H, 4.46. IR (KBr): ν 2106 (s, IrH), 2005 (s, CO), 1484 (m), 1434 (s), 1372 (m), 1331 (w), 1263 (w), 1159 (w), 1096 (s), 1054 (m), 1026, 998 (m), 848 (m), 827 (m), 803 (m), 775 (m), 737 (s), 692 (s), 511 (m), 482 (m), 462 (m) cm^{-1}.^{1}H{^{31}P} NMR (CD_2Cl_2): δ −11.37 (s, 1H, Ir*H*), −9.13 (s, 1H, Ir*H*), 3.05 (d, 1H, C*H*$_2$), 3.16 (d, 1H, C*H*$_2$), 3.30 (d, 1H, C*H*$_2$), 3.70 (d, 1H, C*H*$_2$), 5.24 (d, 1H, C*H*$_2$), 6.04 (d, 1H, C*H*$_2$), 7.29−7.88 (m, 30H, Ar*H*). ^{31}P{^{1}H} NMR (CD_2Cl_2): δ −62.6 (ddd, 1P (P_B), $J_{PP'}$ = 106, 38, 21 Hz), −45.4 (dd, 1P (P_A), $J_{PP'}$ = 267, 38 Hz), −35.2 (dd, 1P (P_C), $J_{PP'}$ = 106, 45 Hz), −12.9 (ddd, 1P (P_D), $J_{PP'}$ = 267, 45, 21 Hz). ESI−MS (CH_2Cl_2): *m/z* 851.199 (*z*1, [Ir(H)$_2$(dpmppm)(CO)]$^+$ (851.151)).

4.6. Preparations of [Ir(H)(SiR$_3$)(meso-dpmppm-κ^3)(CO)]Cl (R$_3$ = Me$_2$Ph (**5a**), HPh$_2$ (**5b**))

For **5a**: To a dichloromethane solution (4 mL) containing **1** (33 mg, 36 μmol) were added Me_2PhSiH (17 μL, 111 μmol) and CH_2Cl_2 (2 mL), and the mixture was stirred at room temperature overnight. The solvent was removed under reduced pressure, and the residue was washed with Et_2O, and extracted with CH_2Cl_2 (6 mL). The extract was passed through a membrane filter and was concentrated to ca. 4 mL, to which diethyl ether (0.5 mL) was carefully added. The solution was kept at 2 °C to give colorless crystals of **5a**, which were separated by filtration, washed with diethyl ether, and dried under vacuum (10 mg, 28%). Anal. Calc. for $C_{48.5}H_{49}OP_4Cl_2Ir$ (**5a**·0.5CH_2Cl_2 (1063.011)): C, 54.80; H, 4.65. Found: C, 54.45; H, 5.04. IR (KBr): ν 2099 (s, IrH), 1986 (s, CO), 1484 (m), 1435 (s), 1378 (w), 1239 (w), 1099 (s), 998 (w), 805 (s), 740 (s), 694 (s), 642 (m), 494 (m) cm^{-1}.^{1}H{^{31}P} NMR (CD_2Cl_2): δ −7.41 (d, 1H, Ir*H*), −0.10 (s, 3H, Si*CH*$_3$), −0.07 (s, 3H, Si*CH*$_3$), 2.19 (d, 1H, C*H*$_2$), 2.87 (d, 1H, C*H*$_2$), 4.47 (d, 1H, C*H*$_2$), 5.29 (d, 1H, C*H*$_2$), 5.79 (d, 1H, C*H*$_2$), 5.95 (d, 1H, C*H*$_2$), 6.78−8.11 (m, 35H, Ar*H*). ^{31}P{^{1}H} NMR (CD_2Cl_2): δ −60.5 (ddd, 1P (P_B), $J_{PP'}$ = 92, 45, 27 Hz), −43.9 (dd, 1P (P_A), $J_{PP'}$ = 266, 45 Hz), −41.1 (dd, 1P (P_C), $J_{PP'}$ = 92, 51 Hz), −16.6 (ddd, 1P (P_D), $J_{PP'}$ = 266, 51, 27 Hz). ESI−MS (CH_2Cl_2): *m/z* 849.239 (*z*1, [Ir(dpmppm)(CO)]$^+$ (849.135)), 985.330 (*z*1, [Ir(H)(SiMe$_2$Ph)(dpmppm)(CO)]$^+$ (985.206)).

For **5b**: By a procedure similar to that of **5a**, using Ph_2SiH_2 instead of Me_2PhSiH, **5b** was obtained in 62% yield. Anal. Calc. for $C_{52.25}H_{48.5}OP_4Cl_{1.5}Ir$ (**5b**·0.25CH_2Cl_2 (1089.821)): C, 57.58; H, 4.49. Found: C, 57.24; H, 4.65. IR (KBr): ν 2103 (s, IrH), 1993 (s, CO), 1485 (m), 1435 (s), 1376 (w), 1315 (w), 1098 (s), 999 (w), 819 (s), 738 (s), 692 (s), 490 (m) cm^{-1}.^{1}H{^{31}P} NMR (CD_2Cl_2): δ −7.20 (s, 1H, Ir*H*), 2.56 (d, 1H, C*H*$_2$), 2.88 (d, 1H, C*H*$_2$), 4.29 (d, 1H, C*H*$_2$), 4.86 (s, 1H, Si*H*), 5.34 (d, 1H, C*H*$_2$), 5.83 (d, 1H, C*H*$_2$), 5.95 (d, 1H, C*H*$_2$), 6.76−8.16 (m, 40H, Ar*H*). ^{31}P{^{1}H} NMR (CD_2Cl_2): δ −61.6 (ddd, 1P (P_B), $J_{PP'}$ = 88, 46, 26 Hz), −50.2 (dd, 1P (P_A), $J_{PP'}$ = 263, 46 Hz), −39.6 (dd, 1P (P_C), $J_{PP'}$ = 88, 50 Hz), −18.5 (ddd, 1P (P_D), $J_{PP'}$ = 263, 50, 26 Hz). ESI−MS (CH_2Cl_2): *m/z* 849.192 (*z*1, [Ir(dpmppm)(CO)]$^+$ (849.135)), 1033.284 (*z*1, [Ir(H)(SiHPh$_2$)(dpmppm)(CO)]$^+$ (1033.206)).

4.7. X-ray crystallographic analysis

The crystals of **3a**·2CH_3CN, **4**·1.5CH_2Cl_2, **5a**·1.5CH_2Cl_2, and **5b**·1.5CH_2Cl_2 were quickly coated with Paratone N oil and mounted

on top of a loop fiber at room temperature. Crystal and experimental data are summarized in Tables S1 and S2. All data were collected at −120 °C on a Rigaku VariMax Mo/Saturn CCD diffractometer equipped with graphite-monochromated Mo Kα radiation using a rotating-anode X-ray generator RA-Micro7 (50 kV, 24 mA). A total of 720–2160 oscillation images, covering a whole sphere of $6° < 2\theta < 55°$ were collected by the ω–scan method ($-70° < \omega < 110°$ (**3a**, **4**, and **5a**), $-62° < \omega < 118°$ (**5b**)) with $\Delta\omega$ of 0.25° or 0.50°. The crystal-to-detector (70 × 70 mm) distance was set at 45 mm (**3a**, **4**, and **5a**) or 60 mm (**5b**). The data were processed using the *Crystal Clear 1.3.5* program (Rigaku/MSC) [81] and corrected for Lorentz–polarization and absorption effects [82] The structures of the complexes were solved by direct methods with *SHELXLS-97* [83] (**4**) and SIR-97 [84] (**3a**, **5a**, and **5b**), and were refined on F^2 with full-matrix least-squares techniques with *SHELXL-97* [83] using *Crystal Structure 4.0* package [85]. All non-hydrogen atoms were refined with anisotropic thermal parameters, and the C–H hydrogen atoms were calculated at ideal positions and refined with riding models. The hydride H atoms of **3a** and **5a** were determined by difference Fourier (DF) syntheses and were refined with isotropic temperature factors, and those of **4** were also found in DF maps and were refined with appropriate thermal parameters. The Ir–H and Si–H hydrogen atoms of **5b** were determined by DF syntheses and were refined as riding models with appropriate B_{iso}. All calculations were carried out on a Windows PC with *Crystal Structure 4.0* package [85].

CCDC 1894233–1894236 contain the supplementary crystallographic data for this paper. These data can be obtained free of charge from The Cambridge Crystallographic Data Center via www.ccdc.cam.ac.uk/data_request/cif.

Acknowledgement

This work was supported by a Grant-in-Aid for Scientific Research (no. 18H03914) and on Priority Area 2802 (no. 17H05374) from the Ministry of Education, Culture, Sports, Science and Technology, Japan. The authors thank Prof. Kohtaro Osakada of Tokyo Institute of Technology for help in MS spectral measurements.

Appendix A. Supplementary data

Supplementary data to this article can be found online at https://doi.org/10.1016/j.jorganchem.2019.03.010.

References

[1] G. van Koten, D. Milstein (Eds.), Organometallic Pincer Chemistry, Springer, Verlag Berlin Heidelberg, 2013.
[2] K.J. Szabo, O.F. Wendt (Eds.), Pincer and Pincer-type Complexes, Wiley-VCH, Weinheim, Germany, 2014.
[3] D. Morales-Morales (Ed.), Pincer Compounds – Chemistry and Applications, Elsevier, Amsterdam, 2018.
[4] R.C. Bauer, Y. Gloaguen, M. Lutz, J.N.H. Reek, B. de Bruin, J.I. van der Vlugt, Dalton Trans. 40 (2011) 8822 (and references cited therein).
[5] M. Mazzeo, M. Strianese, O. Kühl, J.C. Peters, Dalton Trans. 40 (2011) 9026.
[6] A.M. Poitras, S.E. Knight, M.W. Bezpalko, B.M. Foxman, C.M. Thomas, Angew. Chem. Int. Ed. 57 (2018) 1497.
[7] H. Valdès, L. Gonzáles-Sebastián, D. Morales-Morales, J. Organomet. Chem. 845 (2017) 229.
[8] K. Arashiba, E. Kinoshita, S. Kuriyama, A. Eizawa, K. Nakajima, H. Tanaka, K. Yoshizawa, Y. Nishibayashi, J. Am. Chem. Soc. 137 (2015) 5666.
[9] H. Hou, P.K. Gantzel, C.P. Kubiak, J. Am. Chem. Soc. 125 (2003) 9564.
[10] H. Hou, P.K. Gantzel, C.P. Kubiak, Organometallics 22 (2003) 2817.
[11] K.D. John, K.V. Salazar, B.L. Scott, R.T. Baker, A.P. Sattelberger, Organometallics 20 (2001) 296.
[12] B.S. Hanna, A.D. MacIntosh, S. Ahn, B.T. Tyler, G.T.R. Palmore, P.G. Williard, W.H. Bernskoetter, Organometallics 33 (2014) 3425.
[13] R. Cervantes, J. Tiburcio, H. Torrens, New J. Chem. 39 (2015) 631.
[14] J.A. Feducia, M.R. Gagné, J. Am. Chem. Soc. 130 (2008) 592.
[15] D.L. Nelsen, M.R. Gagné, Organometallics 28 (2008) 950.
[16] J.G. Sokol, C.S. Korapala, P.S. White, J.J. Becker, M.R. Gagné, Angew. Chem. Int. Ed. 50 (2011) 5658.
[17] P. Sevilano, A. Habtemariam, S. Parsons, A. Castiñeiras, J. Chem. Soc. Dalton Trans. (1999) 2861.
[18] S.A. Wander, A. Miedaner, B.C. Noll, R.M. Barkley, D.L. BuBois, Organometallics 15 (1996) 3360.
[19] A.R. Siedle, R.A. Newmark, J. Am. Chem. Soc. 103 (1981) 4947.
[20] R. Goikhman, M. Aizenberg, Y. Ben-David, L.J.W. Shimon, M. Milstein, Oraganometallics 21 (2002) 5060.
[21] L. Dahlenburg, M. Ernst, M. Dartiguenave, Y. Dartiguenave, J. Organomet. Chem. 463 (1993) C8.
[22] P.W. Blosser, J.C. Gallucci, A. Wojcicki, J. Mol. Catal. 224 (2004) 133.
[23] Y. Kim, H. Deng, J.C. Gallucci, A. Wojcicki, Inorg. Chem. 37 (1996) 7166.
[24] Y. Kim, H. Deng, D.W. Meek, A. Wojcicki, J. Am. Chem. Soc. 112 (1990) 2798.
[25] G. Jia, J.C. Gallucci, A.L. Rheingold, B.S. Haggerty, D.W. Meek, Organometallics 10 (1991) 3459.
[26] L. Dahlenburg, C. Prengel, Organometallics 3 (1984) 934.
[27] T.M. Buscagan, P.H. Oyala, J.C. Peters, Angew. Chem. Int. Ed. 56 (2017) 6921.
[28] M. Mazzeo, M. Strianese, O. Kühl, J.C. Peters, Dalton Trans. 40 (2011) 9026.
[29] S. Oh, S. Kim, D. Lee, J. Gwak, Y. Lee, Inorg. Chem. 55 (2016) 12863.
[30] Y.-E. Kim, S. Oh, S. Kim, J. Kim, S.W. Han, Y. Lee, J. Am. Chem. Soc. 137 (2015) 4280.
[31] Y.-E. Kim, J. Kim, Y. Lee, Chem. Commun. 50 (2014) 11458.
[32] C. Martin, S. Mallet-Laderia, K. Miqueu, G. Bouhadir, D. Bourissou, Organometallics 33 (2014) 571.
[33] A.D. Sadow, A. Togni, J. Am. Chem. Soc. 127 (2005) 17012.
[34] A.D. Sadow, J. Haller, L. Fadini, A. Togni, J. Am. Chem. Soc. 126 (2004) 14704.
[35] J.F. Buergler, A. Togni, Organometallics 30 (2011) 4742.
[36] R.C. Bauer, Y. Gloaguen, M. Lutz, J.N.H. Reek, B. de Bruin, J.I. van der Vlught, Dalton Trans. 40 (2011) 8822 (and references cited therein).
[37] A.M. Poitras, S.E. Knight, M.W. Bezpalko, B.M. Foxman, C.M. Thomas, Angew. Chem. Int. Ed. 57 (2018) 1497.
[38] B. Pan, D.A. Evers-McGregor, M.W. Bezpalko, B.M. Foxman, C.M. Thomas, Inorg. Chem. 57 (2013) 9583.
[39] B. Pan, M.W. Bezpalko, B.M. Foxman, C.M. Thomas, Organometallics 30 (2011) 5560.
[40] M.J. Ray, R.A.M. Randall, K.S.A. Arachchige, A.M.Z. Slawin, M. Bühl, T. Lebl, P. Kilian, Inorg. Chem. 52 (2013) 4346.
[41] G. Dyer, J. Roscoe, Inorg. Chem. 35 (1996) 4098.
[42] S. Affandi, J.H. Nelson, J. Fischer, Inorg. Chem. 28 (1989) 4536.
[43] P.E. Sues, A.J. Lough, R.H. Morris, J. Am. Chem. Soc. 136 (2014) 4746.
[44] Y. Takemura, H. Takenaka, T. Nakajima, T. Tanase, Angew. Chem. Int. Ed. 48 (2009) 2157.
[45] Y. Takemura, T. Nakajima, T. Tanase, Eur. J. Inorg. Chem. (2009) 4820.
[46] Y. Takemura, T. Nakajima, T. Tanase, Dalton Trans. (2009) 10231.
[47] Y. Takemura, T. Nishida, B. Kure, T. Nakajima, M. Iida, T. Tanase, Chem. Eur J. 17 (2011) 10528.
[48] A. Yoshii, H. Takenaka, H. Nagata, S. Noda, K. Nakamae, B. Kure, T. Nakajima, T. Tanase, Organometallics 31 (2012) 133.
[49] T. Tanase, S. Hatada, A. Mochizuki, K. Nakamae, B. Kure, T. Nakajima, Dalton Trans. 42 (2013) 15941.
[50] T. Tanase, R. Otaki, T. Nishida, H. Takenaka, Y. Takemura, B. Kure, T. Nakajima, Y. Kitagawa, T. Tsubomura, Chem. Eur J. 20 (2014) 1577.
[51] K. Nakamae, B. Kure, T. Nakajima, Y. Ura, T. Tanase, Chem. Asian J. 9 (2014) 3106.
[52] T. Tanase, A. Yoshii, R. Otaki, K. Nakamae, Y. Mikita, B. Kure, T. Nakajima, J. Organomet. Chem. 797 (2015) 37.
[53] K. Nakamae, Y. Takemura, B. Kure, T. Nakajima, Y. Kitagawa, T. Tanase, Angew. Chem. Int. Ed. 54 (2015) 1016.
[54] T. Tanase, S. Hatada, S. Noda, H. Takenaka, K. Nakamae, B. Kure, T. Nakajima, Inorg. Chem. 54 (2015) 8298.
[55] T. Tanase, K. Morita, R. Otaki, K. Yamamoto, Y. Kaneko, K. Nakamae, B. Kure, T. Nakajima, Chem. Eur J. 23 (2017) 524.
[56] T. Nakajima, Y. Kamiryo, K. Hachiken, K. Nakamae, Y. Ura, T. Tanase, Inorg. Chem. 57 (2018) 11005.
[57] T. Nakajima, S. Kurai, S. Noda, M. Zouda, B. Kure, T. Tanase, Organometallics 31 (2012) 4283.
[58] T. Nakajima, M. Sakamoto, S. Kurai, B. Kure, T. Tanase, Chem. Commun. 49 (2013) 5239.
[59] T. Nakajima, S. Noda, M. Sakamoto, A. Matsui, K. Nakamae, B. Kure, Y. Ura, T. Tanase, Dalton Trans. 45 (2016) 4747.
[60] K. Nakamae, T. Nakajima, Y. Ura, Y. Kitagawa, T. Tanase, (to be submitted for publication).
[61] T. Tanase, M. Urabe, N. Mori, S. Hatada, S. Noda, H. Takenaka, K. Nakamae, T. Nakajima, J. Organomet. Chem. 879 (2019) 47.
[62] J.D. Smith, J.R. Logan, L.E. Doyle, R.J. Burford, S. Sugawara, C. Ohnita, Y. Yamamoto, W.E. Piers, D.M. Spasyuk, J. Borau-Garcia, Dalton Trans. 45 (2016) 12669.
[63] L.M. Guard, T.J. Hebden, D.E. Linn Jr., D.M. Heinekey, Organometallics 36 (2017) 3104.
[64] W.-C. Shih, O.V. Ozerov, Organometallics 36 (2017) 228.
[65] M. Iglesias, A. Iturmendi, P.J.S. Miguel, V. Polo, J.J. Pérez-Torrente, L.A. Pro, Chem. Commun. 51 (2015) 12431.
[66] E. Súarez, P. Plou, D.G. Gusev, M. Martin, E. Sola, Inorg. Chem. 56 (2017) 7190.
[67] D.C. Babbini, V.M. Iluc, Oragnometallics 34 (2015) 3141.

[68] J.M. Goldberg, S.D.T. Cherry, L.M. Guard, W. Kaminsky, K.I. Goldberg, D.M. Heinekey, Organometallics 35 (2016) 3546.
[69] J.M. Goldberg, G.W. Wong, K.E. Brastow, W. Kaminsky, K.I. Goldberg, D.M. Heinekey, Organometallics 34 (2015) 753.
[70] J.J. Adams, N. Arulsamy, D.M. Roddick, Organometallics 30 (2011) 697.
[71] B. Rybtchinski, Y. Ben-David, D. Milstein, Organometallics 16 (1997) 3786.
[72] M.A. Esteruelas, M. Oliván, A. Vélez, Inorg. Chem. 52 (2013) 12108.
[73] E. Calimano, T.D. Tilly, Dalton Trans. 39 (2010) 9250.
[74] T. T. MetsäP. Hrobárik, H.F.T. Klare, M. Kaupp, M. Oestreich, J. Am. Chem. Soc. 136 (2014) 6912.
[75] P.P. Deutsch, R. Eisenberg, Chem. Rev. 88 (1988) 1147.
[76] B.J. Rappoli, T.S. Janik, M.R. Churchill, J.S. Thompson, J.D. Atwood, Organometallics 7 (1988) 1939.
[77] M.K. Hays, R. Eisenberg, Inorg. Chem. 30 (1991) 2623.
[78] G. Winkhaus, H. Singer, Chem. Ber. 99 (1966) 3610.
[79] K. Vrieze, J.P. Collman, C.T. Sears Jr., M. Kubota, Inorg. Synth. 11 (1968) 101.
[80] J.W. Kang, K. Moseley, P.M. Maitlis, J. Am. Chem. Soc. 91 (1969) 5970.
[81] Crystal Clear, Version 1.3.5, Operating Software for the CCD Detector System, Rigaku and Molecular Structure Corp., Tokyo, Japan and The Woodlands, Texas, 2003.
[82] R. Jacobson, REQAB, Molecular Structure Corporation, the Woodlands, Texas, USA, 1998.
[83] G.M. Sheldrick, SHELXS-97 and SHELXL-97: Program for the Solution and the Refinement of Crystal Structures, University of Göttingen, Göttingen, Germany, 1996.
[84] A. Altomare, M. Burla, M. Camalli, G. Cascarano, C. Giacovazzo, A. Guagliardi, A. Moliterni, G. Polidori, R. Spagna, J. Appl. Crystallogr. 32 (1999) 115.
[85] Crystal Structure 4.0, Crystal Structure Analysis Package, Rigaku Corporation, Tokyo, 2000-2010, 196-8666, Japan.